



Effects of diagenetic processes on the velocity evolution in carbonate reservoirs

Mohammad Hossein Khosravi ·
Mohammad Emami Niri ·
Mohammad Reza Saberi

Received: 18 November 2022 / Accepted: 26 October 2023
© The Author(s) 2023

Abstract Carbonate rocks are geologically complex due to the diagenetic processes they experience before and after lithification. Diagenetic processes alter their matrix and pore structure leading to the modification in their sonic velocities. Understanding the effect of these diagenetic features on the seismic velocities is crucial to have a reliable image of the subsurface. The dataset used in this study comprises well logs, and core data. Core data were analyzed using different methods (i.e., thin section analysis, X-ray diffraction (XRD) analysis, and scanning electron microscopy (SEM images)) to investigate the presence or absence of different diagenetic processes in each depth interval of the Sarvak formation. In order to minimize porosity effects on velocity variations, we divided all porosity data into five equal porosity classes and performed bar chart analysis in each class. The results indicated that bioturbation (through stiff pore creation and infilling with stiff minerals) and compaction

(through pore space volume reduction) increase velocities, but dissolution increased velocities only for the low porosity samples (through moldic and vuggy pores creation) while reduced it in the high porosity samples (through the interconnection of the isolated pores). Furthermore, porosity enhancement (through increasing pore space volume), micritization (through porosity reduction inhibition during compaction), open fracture (through creation of soft pores and cracks), and neomorphism (through the creation of microporosity during compaction) reduce sonic velocities.

Article Highlights

- The study examines the impact of diagenetic processes on sonic velocities in carbonate rocks using data from four wells in southwest Iran.
- The results reveal new insights into the inverse relationship between micritization, open fracturing, neomorphism, and porosity increase on velocity, compared to the impact of bioturbation and compaction.
- The study highlights the complex relationship between dissolution and velocity, showing that its impact depends on the porosity of the samples.

M. H. Khosravi
School of Mining Engineering, College of Engineering,
University of Tehran, Tehran, Iran

M. Emami Niri (✉)
Institute of Petroleum Engineering, School of Chemical
Engineering, College of Engineering, University
of Tehran, Tehran, Iran
e-mail: Emami.m@ut.ac.ir

M. R. Saberi
Geosoftware, The Hague Area, 2591 XR The Hague,
The Netherlands

Keywords Diagenetic processes · Carbonates ·
Velocity evolution · Porosity · Pore types

1 Introduction

Carbonate rocks are subjected to various diagenetic processes following deposition, which can significantly alter their porosity, pore types, and ultimately impact their elastic properties and seismic responses. Understanding the effects of these diagenetic features on the rock microstructure and elastic properties is crucial for accurately interpreting velocities and seismic data. While several studies have investigated the impact of diagenetic processes and different parameters on carbonate velocity variations (Anselmetti and Eberli 1993; Emami Niri et al. 2021; Khosravi et al. 2022; Saberi 2020; Salih et al. 2021a, b), there are still some diagenetic processes whose effects remain uncertain or unknown.

Anselmetti and Eberli (1993) conducted comprehensive laboratory experiments to measure the velocities of compressional and shear waves in 210 carbonate cores from diverse areas and ages, under various laboratory conditions. Their findings indicated that changes in mineralogy were not solely responsible for the significant velocity variations observed (Anselmetti and Eberli 1993). Additionally, they observed that shallow marine environment deposits exhibited higher average velocities compared to deep-water deposits, suggesting a lower diagenetic potential for deep-water carbonates (Anselmetti and Eberli 1993).

Fabricius (2003) developed an elastic model to investigate the influence of burial diagenesis on acoustic velocity and porosity in chalk sediments. The study revealed that cementation of young deep-sea sediments increased velocity without affecting porosity (Fabricius 2003). Furthermore, dissolution processes in carbonate formations were found to result in pore space cementation, leading to increased velocities (Fabricius 2003).

Brigaud et al. (2010) conducted laboratory research on more than 250 carbonate core plugs and found that compacted rocks without early cementation exhibited higher sonic velocities than rocks with early cementation. Matonti et al. (2015) investigated the impact of stylolite and open fractures on carbonate velocities and observed significant reductions in velocity. El Husseiny and Vanorio (2015) studied the influence of micrite presence on carbonate sonic velocities and found that micritization strengthened the rock, resulting in increased acoustic velocity.

Jafarian et al. (2017) analyzed the dependency of different parameters on the acoustic velocity of mixed carbonate and non-carbonate rocks. Their study demonstrated that variations in velocity primarily arose from the mineral composition in mixed lithology samples (Jafarian et al. 2017). Dolomitization was observed to increase velocities in dolostone compared with limestone samples. Porosity and bulk density were ranked as the second and third parameters affecting velocities, respectively (Jafarian et al. 2017).

Jaballah et al. (2021) analyzed the physical properties of outcrop carbonate samples and observed that dolomitization reduced velocities by creating intercrystalline pores, while neomorphism and cementation increased velocities by making the rock stiffer. Salih et al. (2021a, b) investigated the diagenetic controls on sonic velocity in the Khuff carbonate formation through modeling and core measurements. Dolomitization was found to reduce velocity by developing interconnected pores and increasing permeability (Salih et al. 2021b). Dissolution processes generated high aspect ratio moldic and vuggy pores, resulting in an increase in velocity (Salih et al. 2021b). They also studied the impact of bioturbation on acoustic velocities in bioturbated carbonate samples and found that the presence of burrow fill had distinguishable effects on velocity variations, with coarse grain-filled burrows exhibiting lower velocities than fine grain-filled burrows (Salih et al. 2021b).

While there have been prior investigations into certain diagenetic processes such as cementation, dissolution, compaction, fracture, micritization, bioturbation, neomorphism, and dolomitization in relation to acoustic velocities, additional research is needed to explore these processes comprehensively. This study aims to examine the influence of several diagenetic features, including dissolution, compaction, fracturing, micritization, bioturbation, and neomorphism, on the sonic velocity of carbonate rocks. To achieve this, we utilize an extensive dataset obtained from four wells in the Sarvak formation of a carbonate oilfield in southwest Iran. The dataset includes well logs and core samples, which have been analyzed through thin section analysis, SEM imaging, and XRD analysis to determine mineralogy, textures, and dominant diagenetic features. In this study, we employ a novel bar chart analysis approach to evaluate the influences of mineralogy, porosity, and various diagenetic processes on the measured log sonic velocities. By

addressing these knowledge gaps, our research aims to enhance the understanding of the intricate relationship between diagenesis and rock velocities in carbonate reservoirs.

1.1 Geological setting

The study area, Abadan plain, is located in the southwest of Iran, where the most significant oilfields of Iran are placed. (Fig. 1). The Abadan plain is surrounded by the Zagros fold-thrust belt (ZFTB) in the northeast and the Arabian shield in the southwest (Assadi et al. 2016; Mehrabi et al. 2015). Therefore, its structural and geological characteristics are

influenced by both regions. However, the impacts of the Arabian shield are more significant in the geological and structural features of the Abadan plain (Assadi et al. 2016; Mehrabi et al. 2015). Hence, the structure trend is N-S (Arabian plate trend), contrasting with the Zagros trend (NE-SW) (Fig. 1) (Assadi et al. 2016). Formations with reservoir potential in the Abadan plain are the Bangestan (Sarvak and Ilam) and Khami (Fahliyan and Gadvan) groups (Assadi et al. 2018), which Sarvak is the target Formation of this study. Figure 2 shows a generalized stratigraphic column of the Abadan plain.

Sarvak formation, which has deposited in the middle cretaceous, is the second most significant

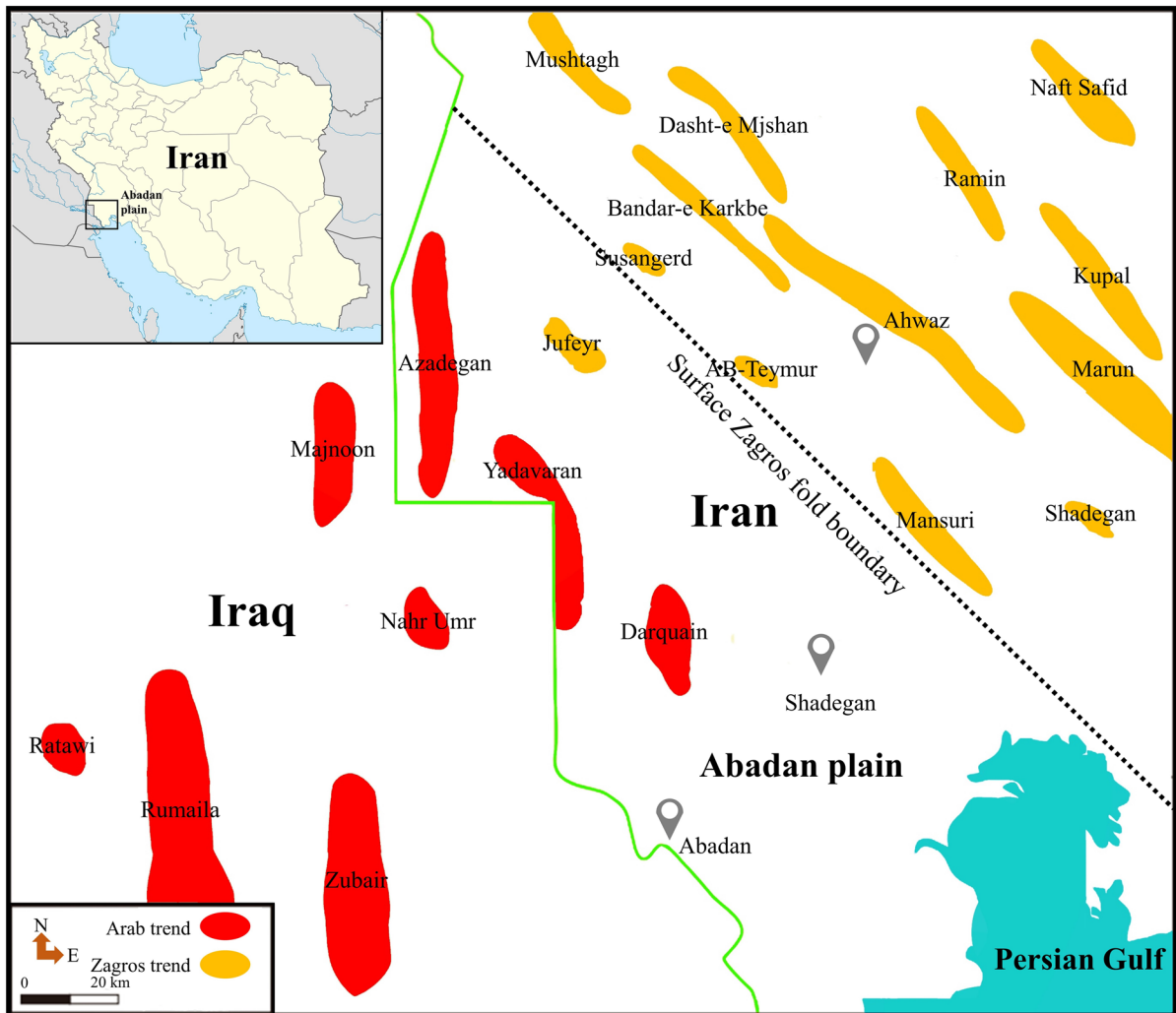
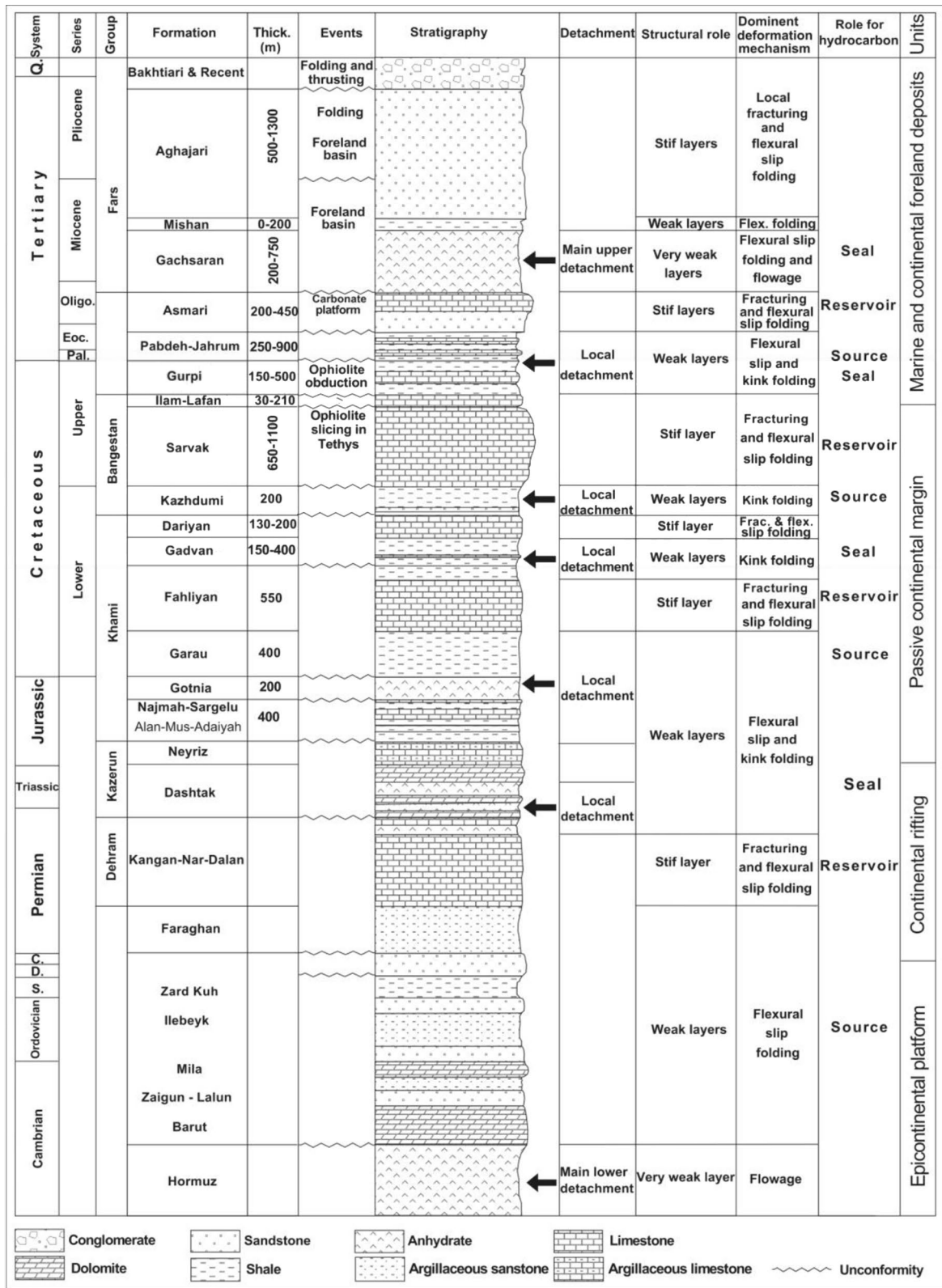


Fig. 1 Regional location map of the Abadan plain in southwest of Iran (Reproduced from Du et al. (2016))



◀**Fig. 2** A simplified representation of the geological section and significant tectonic events that occurred in the Abadan plain

reservoir formation in Iran after Asmari Formation (Esrafil-Dizaji et al. 2015; Jooybari and Rezaie 2017). This formation has an approximate thickness of 820 m at the type section (Tange Sarvak, Kuh-e Bangestan) (Esrafil-Dizaji et al. 2015; James and Wynd 1965). However, its thickness is almost 700 m in the study wells of this study. Generally, Ilam Formation overlaid Sarvak formation in Zagros, but there is a thin argillaceous shaly limestone formation named Laffan between these two formations in the Abadan plain (Assadi et al. 2016, 2018; Mehrabi et al. 2015; Rahimpour-Bonab et al. 2012a, 2012b). In the Abadan plain, the Laffan, with a thickness of 10–15 m, formed a cap rock for the Sarvak formation (Assadi et al. 2018; Mehrabi et al. 2015).

The age of the Sarvak formation is from the late Albian to the middle Turonian (James and Wynd 1965; Motiei 1993; Setudehnia 1978). In the study area, three unconformities (disconformities) have been identified in the Sarvak interval including (a) mid-Cenomanian, (b) Cenomanian–Turonian, and (c) mid-Turonian (top of the formation) (Assadi et al. 2016; Mehrabi et al. 2015; Rahimpour-Bonab et al. 2012a, b). Based on the existing unconformities, Sarvak formation is divided into three portions: (a) lower (between late Albian and middle Cenomanian disconformity), middle (middle Cenomanian to Cenomanian–Turonian disconformity), and upper (between Cenomanian–Turonian and middle Turonian disconformities) (Mehrabi et al. 2015; Rahimpour-Bonab et al. 2012a, b). Lower and middle Sarvak have deposited in a carbonate ramp, while upper Sarvak has formed in a carbonate shelf sedimentary environment (Assadi et al. 2016).

Lower Sarvak is placed on the Kazhdomi Formation (late Albian), and its upper boundary is middle Cenomanian disconformity. In the middle Cenomanian, the sea level dropped, leading to a wide exposure of the basin and middle Cenomanian disconformity formation (Grélaud et al. 2010; Rahimpour-Bonab et al. 2012a, b). The dissolution process signs are observed in the unconformity surface (Assadi et al. 2016). After that, the sea level increased again, and middle Sarvak deposited on the middle Cenomanian disconformity (Rahimpour-Bonab et al.

2012a, b). Then, the exposure of the middle Sarvak and its uppermost part erosion occurred between the late Cenomanian and early Turonian due to salt diapirism and the reactivation of the basement faults (Assadi et al. 2016; Rahimpour-Bonab et al. 2012a, b). The meteoric dissolution process enhanced the porosity and permeability in this period; hence the uppermost of the middle Sarvak is the best reservoir zone of this formation (Assadi et al. 2016; Du et al. 2016; Rahimpour-Bonab et al. 2012a, b). In addition, bioturbation and recrystallization were also observed below the Cenomanian–Turonian disconformity surface (Assadi et al. 2018). Following that, the sea level highly increased again, resulting in the upper Sarvak accumulation above the Cenomanian Turonian disconformity (Assadi et al. 2016). During the middle Turonian, sea levels globally fell, and severe erosion occurred in the upper Sarvak, leading to middle Turonian disconformity creation (Assadi et al. 2016, 2018). Turonian sediments are mud-dominated, therefore, recrystallization of micrites is a dominant diagenetic feature in these deposits (Assadi et al. 2018).

2 Material and methods

In order to investigate the relationship between carbonate elastic properties and their diagenetic processes, we chose four wells in the aforementioned carbonate platform. Here, various data from different sources like well logs and core samples were used. Furthermore, Core data were analyzed using different methods like thin section analysis, XRD analysis, scanning electron microscope (SEM). This section will give detail insight about these data and methods.

2.1 Well logs data

The well log data including caliper, gamma-ray (CGR and SGR), sonic waves transit times (DT and DTS), Neutron density (NPHI), photoelectric factor (PEF), density (RHOB, DRHO), and resistivity logs (LLD, LLS) in addition to petrophysical evaluations comprising porosity (φ_e), mineral volumes, and fluid saturations, were available for four wells (W1, W2, W3, and W4) in the studied field. The location of these wells is present in Fig. 3. Most of the data mentioned above are available in the formations Gachsaran, Asmari, Pabdeh, Sarvak, Gurpi, and Ilam.

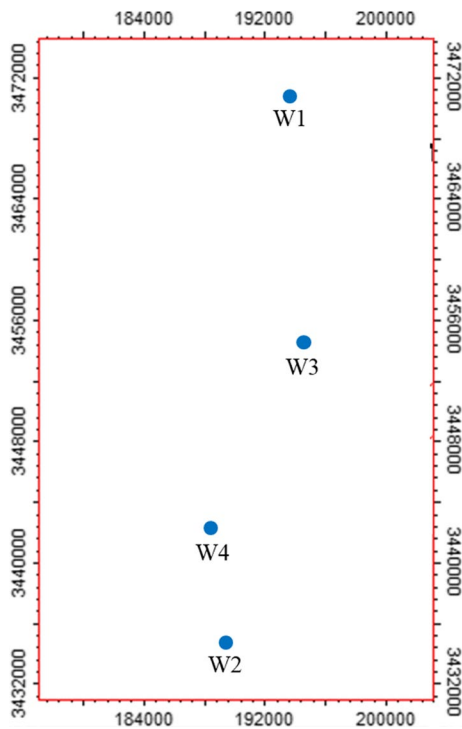


Fig. 3 2D map of the location of the wells examined in this study

Nevertheless, this study focused on the Sarvak zone and the log data of this formation were utilized. Overall, the well log data in the Sarvak interval were of good quality, and there were no sections without data or with noisy data.

2.2 Core data

Core data were not present in the entire Sarvak interval of the investigated wells; therefore, analyses were limited only to the sections with this type of data. Based on the sequence stratigraphy of the Sarvak formation, it is generally divided into 12 subzones (Assadi et al. 2016; Du et al. 2016). These subzones are different in terms of reservoir potential from high (Sar3 and Sar8) to moderate (Sar4-6) and low (Sar1, Sar2, Sar7, Sar9, Sar10, Sar11, and Sar12) porosity and permeability subzones. In terms of facies, various facies (Wackstone, Mudstone, Packstone, Floatstone, and Grainstone) were observed in these subzones. Core data availability at these subzones are shown in Fig. 4. This figure confirms that core data covers around 258 m in W1, 100 m in W2, 180.58 m in

W3, and 53.33 m in W4. These core plugs have gone through the below experiments:

2.2.1 Thin section analysis

Thin section petrography is a type of laboratory experiment that provides information about the microstructure and composition of the rocks (Bullock et al. 1985). In this method, thin sections of the samples are prepared by cutting a thin slice of the rock with a diamond saw and polish optically flat. Then, it is placed on a glass plate and smooth with a progressively finer abrasive grit to reach the desired thickness. We also impregnated blue epoxy into some thin sections to visualize the pore space and stained samples partly with Alizarin red-S to distinguish between calcite and dolomite (Dickson 1966). Two thousand and nineteen thin section samples were prepared to determine diagenetic features and their level of dominance. These thin sections were selected so as to have a uniform distribution of the data in all zone with core samples. Table 1 lists the number of thin section samples provided for each well. After the sample preparation step, samples were analyzed under a polarizing microscope to investigate their predominant diagenetic processes. A number between zero and four was assigned to each diagenetic feature indicating its dominance. Number zero refers to the absence of that process, while number four implies the highest dominance of that diagenetic feature.

2.2.2 XRD analysis

One of the most important tools for analyzing the mineral composition of rocks is using XRD technique. In the XRD analysis, monochromatic X-rays are irradiated on a sample, then the reflected X-ray scattering angles and intensities are measured. A Philips PW 1800 X-ray diffractometer was used for the sample analysis in this study at 40 kV and 30 mA using Cu K α radiation. In this research, around twenty samples were pulverized, and XRD analysis was performed on them. The selection was based on the presence of samples from different subzones of the Sarvak formation. The number of the XRD analyses is listed in Table 1 for each well. The results confirmed that calcite is the main constituent of our studied samples.

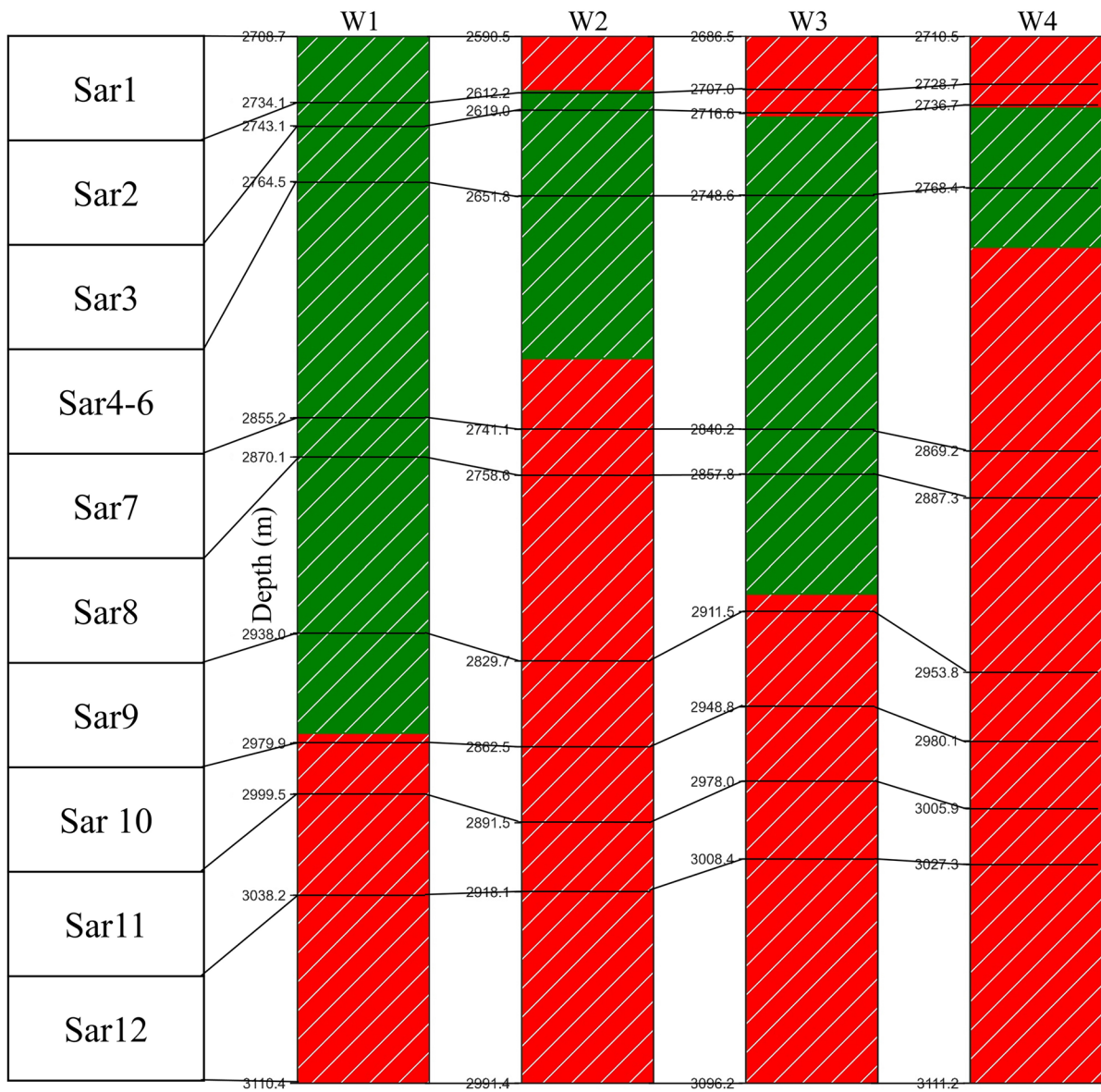


Fig. 4 Core data availability status in the studied wells. Green and red internals indicate depths with and without core data, respectively

Table 1 Number of available data samples in the four studied wells

Data type	Number of data sample				Total
	W1	W2	W3	W4	
Thin sections	907	351	552	209	2019
XRD	6	6	4	4	20
SEM	12	7	18	5	42

2.2.3 SEM images

Scanning electron microscope (SEM) images is a commonly used tool for producing high-resolution magnified images of the surfaces of rocks by using electrons rather than light (Zhou et al. 2007). SEM generate various signals on the surfaces of solid objects by using the focused beam of high-energy electrons (Hafner 2007). Analyzing the signals from

electron-sample interactions makes it possible to determine the microstructure properties of the sample, including texture, crystalline structure, pore and grain shapes etc. The analysis was conducted on the fresh broken surfaces in 20 kV accelerating voltage. In this study, we prepared 42 representative samples for the SEM analysis. Samples for SEM analysis were selected from various reservoir zones, lithologies, depositional textures, and environments to determine their microscopic features. The number of SEM specimens taken from each well is summarized in Table 1. Based on the results, moldic and vuggy porosity were observed in many samples, suggesting that dissolution was the dominant process in these specimens. Moreover, micro-cracks were found in some cases, implying fracturing also occurred there.

2.3 Velocities and diagenetic features relationship analysis

As mentioned above, the presence or absence of different diagenetic processes in each depth interval of the Sarvak formation was determined by examining thin-section data and SEM images. In the next step, the relationship between each diagenetic feature occurrence and sonic velocity variations is explored. This task presents a challenge due to the involvement of multiple complex and interdependent processes, rendering it arduous to ascertain the specific impact of each diagenetic process on sonic velocities. In this process, in order to minimize the effect of porosity

on our analysis, we divided the data into five distinct groups based on their respective porosity values and conducted further analysis for each group separately. The significant impact of extensive changes in porosity on sonic velocities, which obscures the effects of diagenetic processes, is the reason for this grouping approach in our analysis. Porosity calculated during petrophysical evaluation, which is the principal influencing factor on the sonic velocities, has changed between 0 and 23.09%. Therefore, we divided the available data into five classes based on their porosity values (Fig. 5). Then, the relationship between velocity and the given diagenetic features analyzed separately in each porosity group. This will minimize the impact of porosity value on our investigations.

In order to examine the effects of each diagenetic feature on seismic velocities, bar chart analysis is used. In this regard, the velocities in each porosity class (classes one to five in Fig. 5) were divided into three equal groups of low, medium, and high. Partitioning the wide range of velocities into three categories was a pragmatic approach to make the analysis more tractable given the large dataset. It allowed us to discern the influence of diagenetic factors on velocity in a generalized sense, without focusing only on the lower velocity ranges. The ranges of velocity windows for each porosity class were summarized in Table 2. The percentage of samples affected by the diagenetic process, relative to the total examined samples in each velocity interval, was then calculated. Finally, the diagenetic feature percentage for different

Fig. 5 Porosity classes group in the studied samples

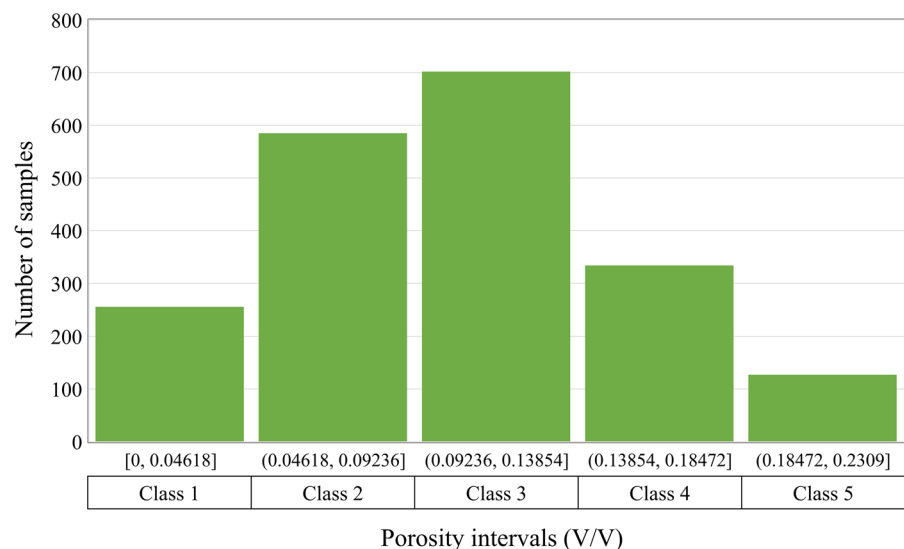


Table 2 The velocity groups for each porosity class

Porosity class name	Porosity ranges (%)	P-wave velocity ranges (m/s)			S-wave velocity ranges (m/s)		
		Low	Medium	High	Low	Medium	High
<i>Class 1</i>	0 to 4.618	3974.22 to 4732.95	4732.95 to 5491.69	5491.69 to 6250.423	2274.10 to 2665.66	2665.66 to 3057.21	3057.21 to 3448.76
<i>Class 2</i>	4.618 to 9.236	3916.28 to 4537.13	4537.13 to 5157.98	5157.98 to 5778.834	2038.84 to 2502.00	2502.00 to 2965.15	2965.15 to 3428.3
<i>Class 3</i>	9.236 to 13.854	4040.27 to 4699.55	4699.55 to 5358.84	5358.84 to 6018.12	1726.63 to 2145.51	2145.51 to 2564.38	2564.38 to 2983.25
<i>Class 4</i>	13.854 to 18.472	3883.30 to 4602.47	4242.88 to 4602.47	4602.47 to 4962.06	1758.33 to 2100.39	2100.39 to 2442.45	2442.45 to 2784.51
<i>Class 5</i>	18.472 to 23.09	3786.21 to 3990.41	3990.41 to 4194.61	4194.61 to 4398.823	1928.98 to 2138.06	2138.06 to 2347.15	2347.15 to 2556.23

velocity intervals was plotted to analyze the impact of each process on the sonic velocities.

3 Results

In this section, the research findings on the factors controlling velocity, including mineralogy, porosity, and different diagenetic processes, are reported. Here, observed velocity variation due to mineralogy and porosity changes are initially reported. Then, the effects of diagenetic processes including bioturbation, compaction, dissolution, micritization, open fracturing, and neomorphism are investigated.

3.1 Mineralogy

In the dataset used for this study, mineralogy variation is not an influencing parameter on the sonic velocities as the reservoir mineralogy is mainly calcite within the Sarvak formation. XRD analysis and thin section images was utilized to determine the mineralogy of the samples. Figure 6 depicts the XRD analysis of a sample from well W4 demonstrating that it is predominantly composed of calcite. Figure 7 displays the mean compositions of all samples analyzed in this study, along with a histogram plot illustrating the distribution of constituent minerals. The prevalence of calcite as the primary mineral is apparent in the majority of the

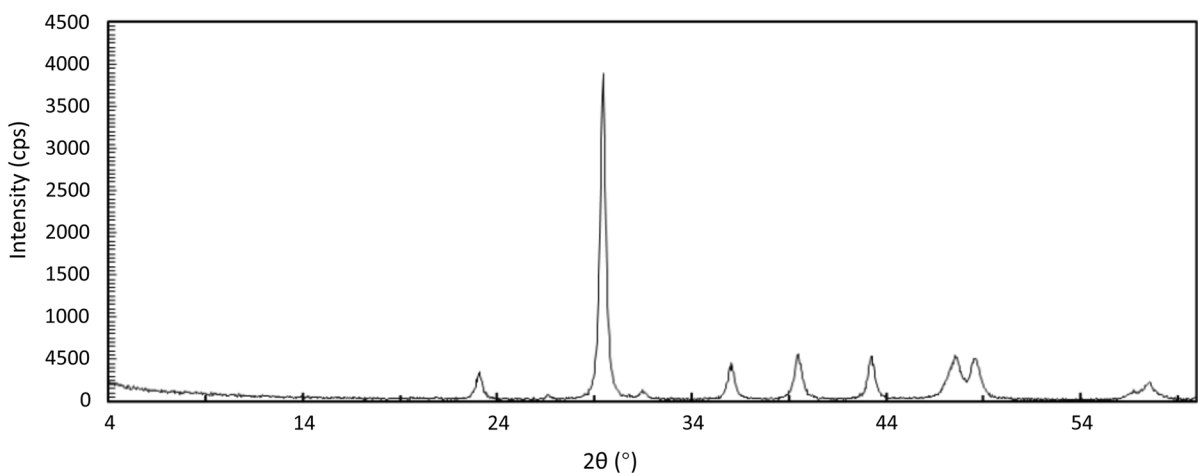


Fig. 6 A typical XRD analysis of a sample from the W4 well at depth 2787.35 m. This analysis reveals that this sample is composed of approximately 3% clay minerals and 97% calcite

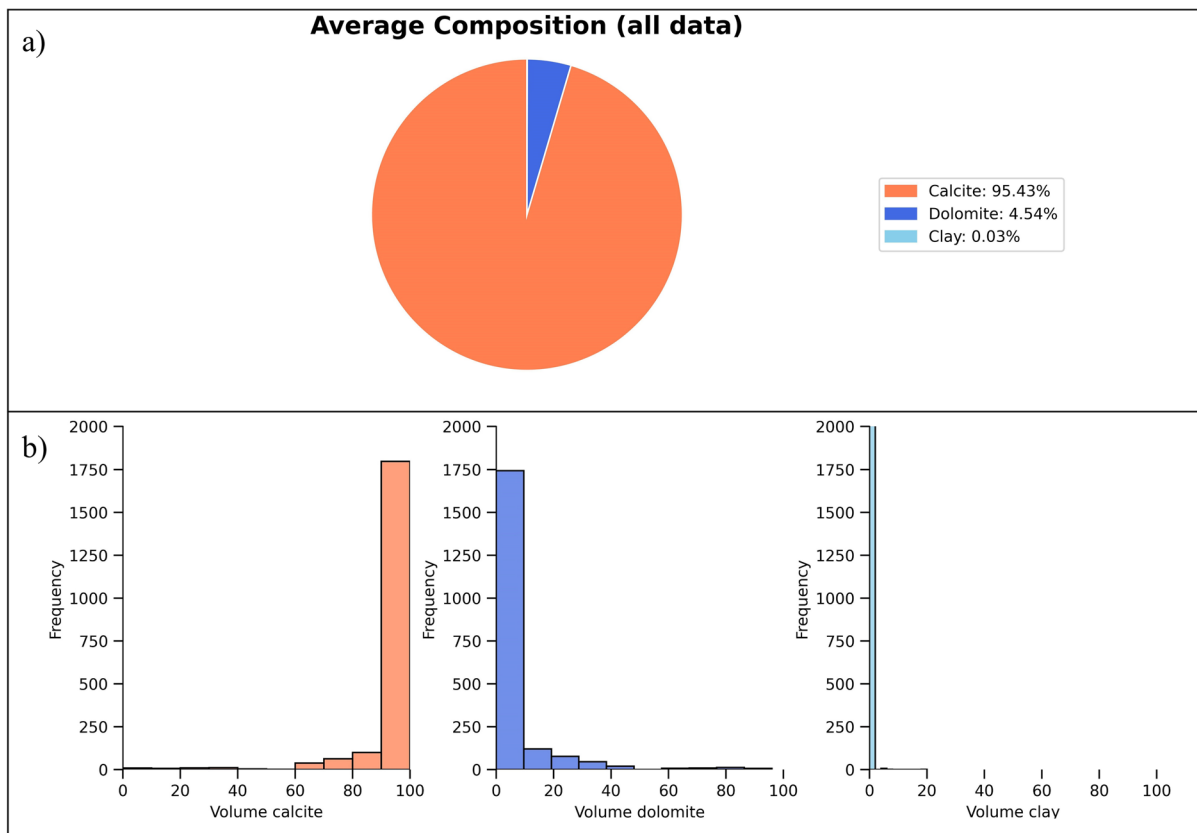


Fig. 7 **a** Average mineral composition, and **b** histogram depicting the volume fractions of the samples examined in the study

samples, with dolomite accounting for only 4.54% of the overall mineral composition. Conversely, clay is not a significant constituent, comprising nearly 0% of the samples' mineralogy. The analysis of the mineral's volume fractions depicted in the histograms indicates that the samples analyzed in this study do not exhibit a substantial concentration of clay. Instead, the predominant minerals observed are calcite and dolomite. According to Mavko et al. (2009), the elastic characteristics of calcite and dolomite exhibit a high degree of similarity. Additionally, the presence of clay in low volume percentages suggests that the matrix component of the rock can be considered to be nearly elastically uniform, with minimal influence on sonic wave velocities. The variations in sonic velocities observed in the sample can be ascribed to the characteristics of the pore space and the geometric properties of the pores, which will be examined in the subsequent section.

3.2 Porosity

Prior studies showed that as the pore space volume (porosity) increases, velocity decreases (Raymer et al. 1980; Wyllie et al. 1956). In order to examine the velocity-porosity relation in the Sarvak formation, we plotted the well log P- and S-wave velocities against porosity log data (Fig. 8). It is evident that velocity and porosity are indirectly related with a high correlation ($R^2_{v_p-\phi} = 0.92$ and $R^2_{v_s-\phi} = 0.84$), indicating that as porosity increases, velocity decreases. S-wave velocity shows less correlation with porosity compared with the P-wave velocity, which can be related to more erroneous S-wave data.

In carbonate rocks, pore geometry can affect sonic wave velocities as much as porosity (Anselmetti and Eberli 1993). Experimental results demonstrated that pore shape could modify

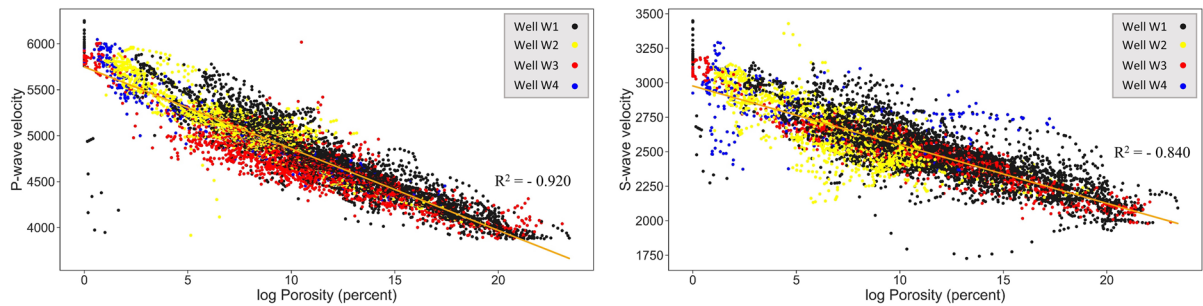


Fig. 8 P-wave and S-wave velocities cross plot against porosity for the four wells' data

P-wave velocity by up to 40% at a certain porosity value (Xu and Payne 2009). In general, pores with a high aspect ratio (close to 1), such as moldic and vuggy pores, cause the sonic velocities to increase in a constant porosity (Xu and Payne 2009). On the other hand, low aspect ratio pores (aspect ratio close to 0) like micro-cracks weaken the rock and reduce its acoustic velocities (Xu and Payne 2009). Different diagenetic processes generate different pore types in carbonate rocks. This can affect their velocity accordingly. In the dataset of this study, pore types have also been interpreted visually from these sections and SEM images. No meaningful relationship between these interpreted pore types and velocity variations was observed. The effects of different pore geometries on sonic velocities during diagenetic processes will be investigated in the following. Different diagenetic processes potentially can generate different pore types, and this can help with a better investigation on velocity changes due to pore geometry changes.

3.3 Bioturbation

This process was observed as a pervasive diagenetic feature in the Sarvak formation (Assadi et al. 2018). The examined specimens have shown a significant amount of bioturbation (Fig. 9). It was mainly recorded as boring features within the large skeletal grains (rudists), which were subsequently filled by fecal pellets, micrite, and cement (Fig. 9b, d). The burrowing filled with peloids and cement was another type of bioturbation that was mainly recognizable in our examined samples (Fig. 9a, c).

Figure 10 depicts the final investigation results of the observed diagenetic features for well W1. It can

be seen that bioturbation within the Sarvak formation varies from zones without this feature to intervals with a high bioturbation dominance. Also, this diagenetic process was more evident in the upper part of the Sarvak formation compared with the lower parts (Fig. 10). We plotted the percentage of the bioturbated samples to all investigated samples in each velocity group (low, medium, and high) for different porosity classes (classes 1 to 5) (Fig. 11). It is evident that as the dominance of bioturbation grows in samples their velocity increase. Therefore, we can conclude that, in general, bioturbation increases both P- and S- wave velocities within all of our porosity groups. This can be attributed to the created stiff pores as well as their stiff filling minerals.

3.4 Compaction

This diagenetic feature was widely observed with high dominance in the Sarvak formation (Fig. 10). Compaction is classified into mechanical and chemical categories, where mechanical compaction occurs just after deposition, and chemical compaction happens in deep burials (Croizé et al. 2013). Mechanical compaction is mainly induced by lithostatic pressure, reducing the bulk volume rock (Croizé et al. 2013). We observed this process in almost all samples from the studied wells (Fig. 12c and d). The main indicators of mechanical compaction in the samples were grain deformation, grain slippage, and rearrangements (Fig. 12c and d). On the other hand, chemical compaction is caused by an increase in solubility at grain contacts and happens along sediment boundaries due to an increase in the applied stress (Croizé et al. 2010). This stress comes from the overburden pressure or sometimes

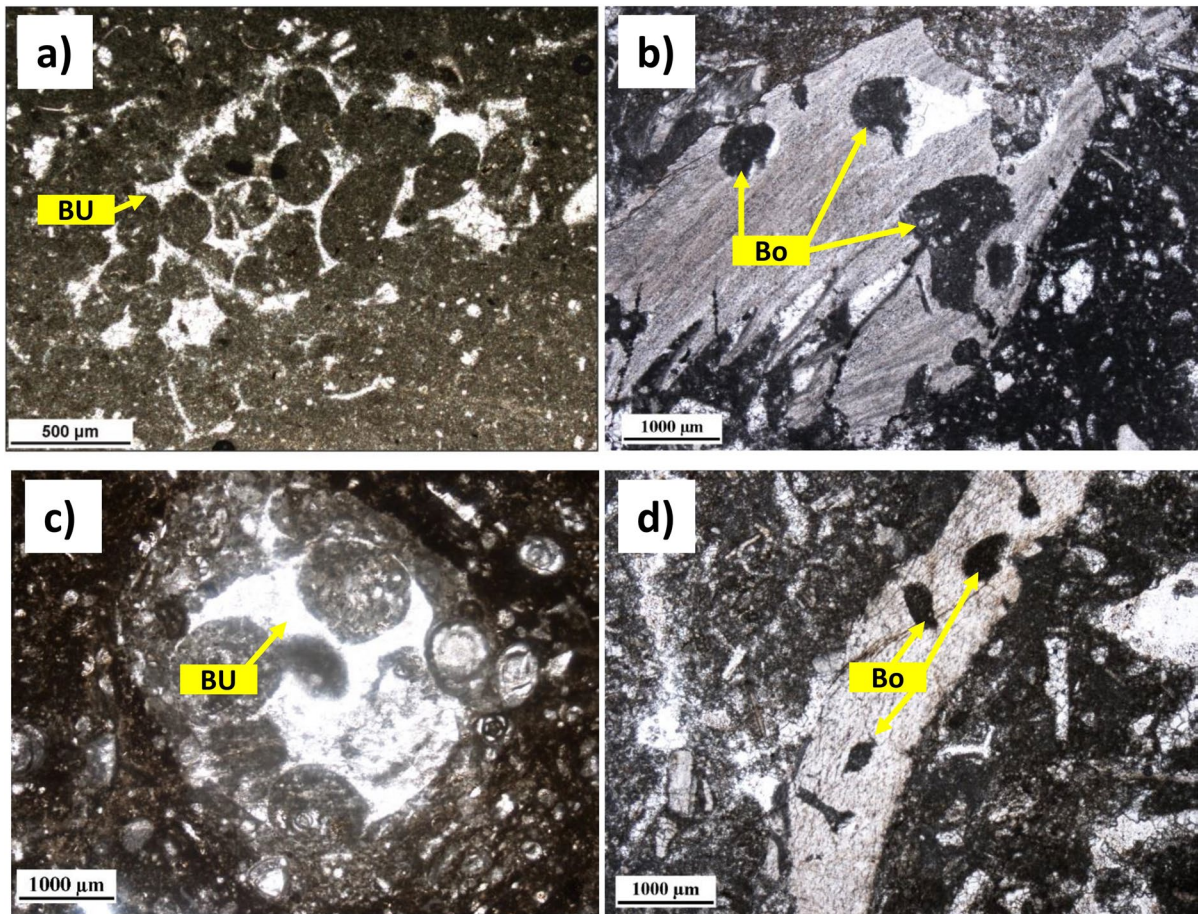


Fig. 9 Photomicrographs of bioturbation in the Sarvak formation. **a** burrow filled with fecal pellets (well W1, depth=2717.61 m), **b** boring of a rudist shell (well W2,

depth=2631.18 m), **c** burrow filled with peloids and cement (well W3, depth=2741.40 m), and **d** boring of a rudist shell (well W4, depth=2751.14 m)

tectonic stresses, which finally will lead to pressure dissolution (Serra 1983). We observed chemical compaction within the Sarvak formation in the forms of solution seams (non-sutured) and stylolite (sutured) (Fig. 12a and b).

In order to examine the effects of the compaction process on velocity variations, similar to bioturbation, bar chart analysis was utilized. Figure 13 shows the results of our investigations for the compaction process. It can be concluded that velocity increases by occurring of the compaction. This is mainly because of porosity reduction during this diagenetic process. Our findings for the compaction feature confirm the result of Brigaud et al. (2010) and Jaballah et al. (2021).

4 Dissolution

Dissolution is a prevalent diagenetic process in carbonate rocks, which was also dominant in our studied formation (Fig. 10). In the upper Sarvak formation (especially in Sar-2 and Sar-3 zones), widespread meteoric dissolution was observed in the form of molds and vugs (Fig. 10). In general, Sarvak formation has undergone two phases of dissolution in most parts of the Zagros area (Assadi et al. 2016, 2018; Du et al. 2016; Mehrabi and Rahimpour-Bonab 2014). It resulted in the generation of two different types of vugs within the Sarvak formation: fabric-selective vugs and touching non-fabric selective vugs. Fabric selective vugs occurred

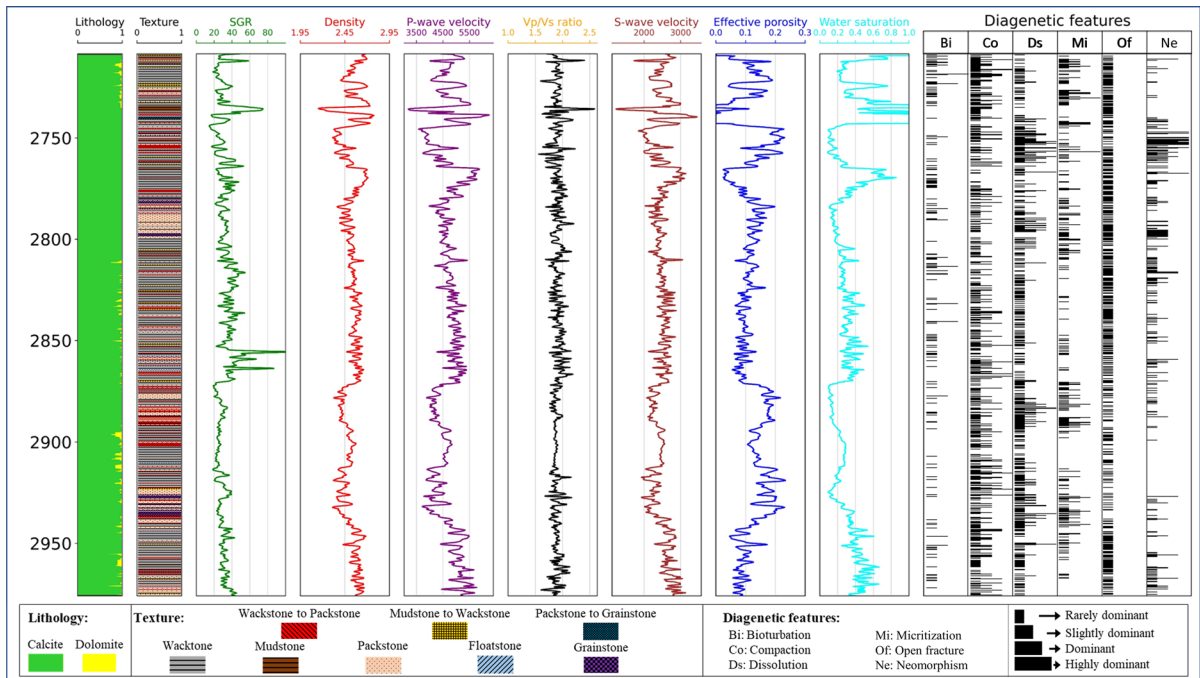


Fig. 10 The columns of lithology, texture, conventional well logs, and diagenetic features dominance in the well W1

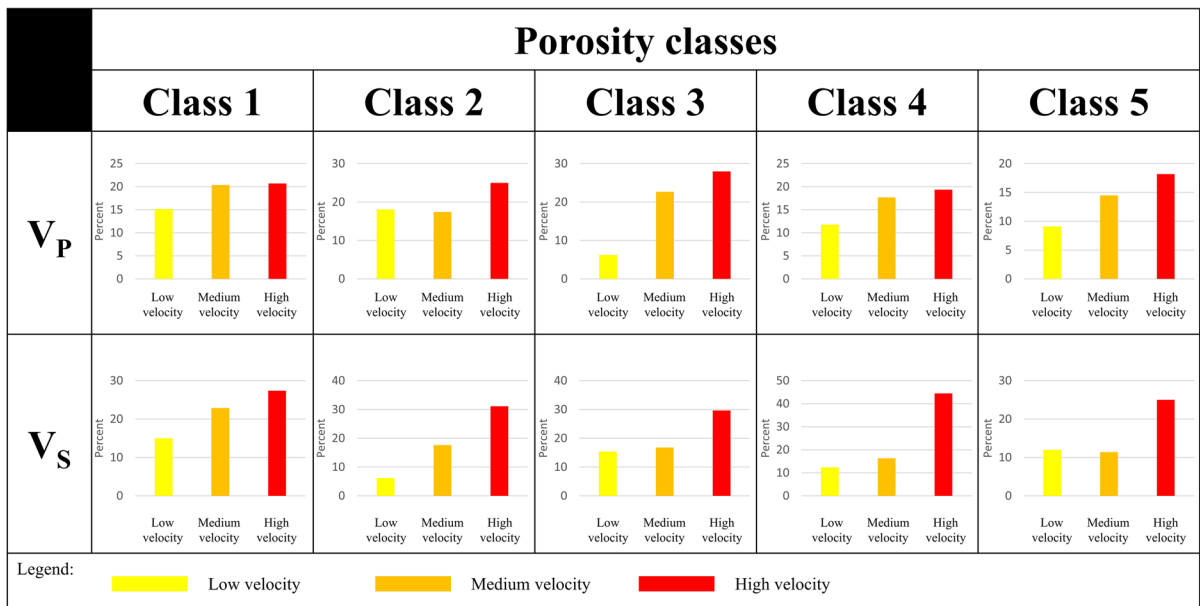


Fig. 11 The percentage of samples that underwent bioturbation to total investigated samples for different velocity groups (low, medium, and high velocities) in each porosity class (classes one to five)

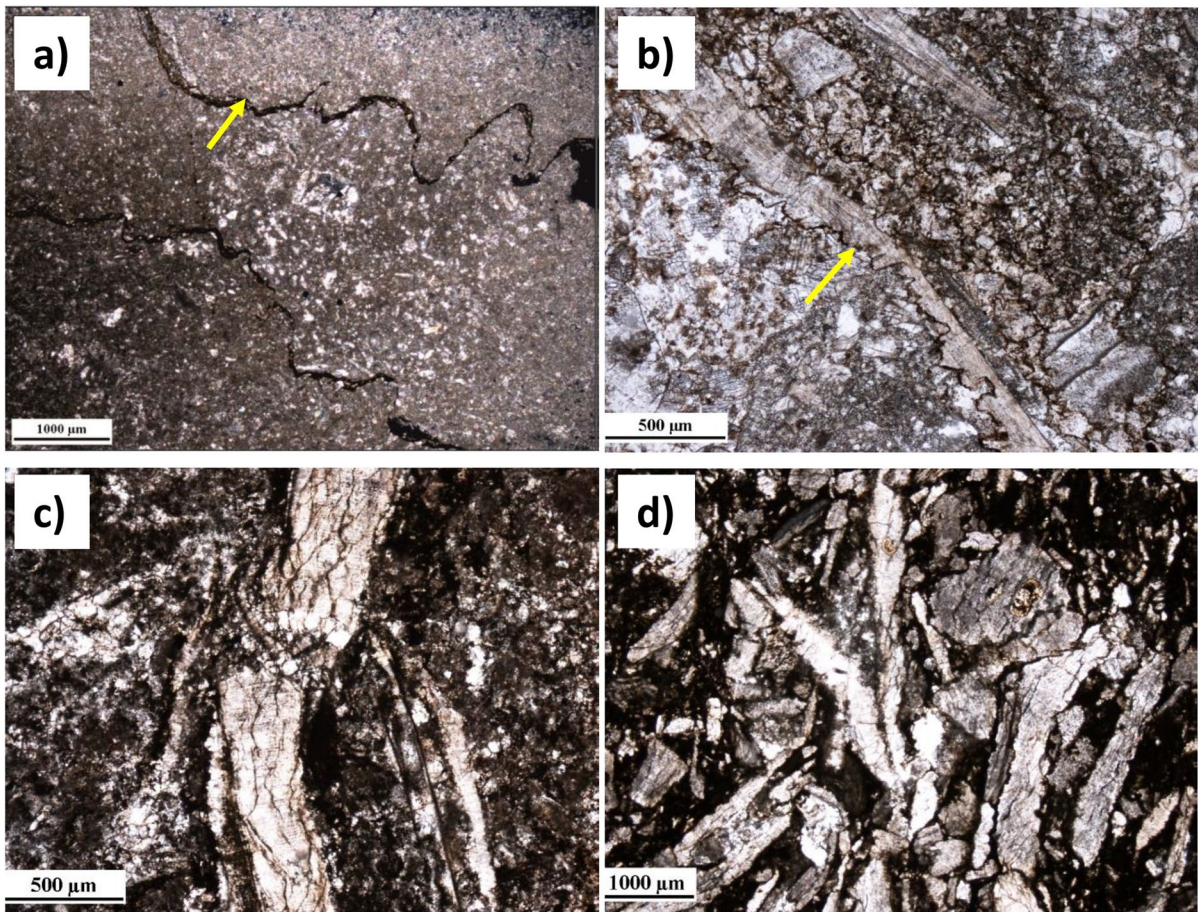


Fig. 12 Photomicrographs of compaction features in the Sarvak formation. **a** Stylolite (well W1, depth=2950.95 m), **b** chemical compaction in the forms of stylolite and solution seams (well W2, depth = 2686.50 m), **c** mechanical compaction

in the form of grains packing (well W3, depth=2720.53 m), and **d** mechanical compaction in the form of grains packing (well W4, depth = 2756.03 m)

following deposition before the sediments were completely lithified. Later, these vugs were filled with meteoric (phreatic) or burial cement. However, some parts of them were partially to fully preserved forming high-quality reservoirs, especially where micro-fractures connected them. Non-fabric selective vugs are formed after lithification, and they are widespread below Cenomanian–Turonian and post-Turonian (top-Sarvak) unconformities within the Sarvak formation (Assadi et al. 2016, 2018; Rahimpour-Bonab et al. 2012a, b). This phase of dissolution creates separate and touching vugs and moldic porosities at the mentioned unconformities. In general, dissolution process caused the generation of stiff (moldic and vuggy) pores in the Sarvak

formation. This process induces moldic and vuggy porosities, which are obvious in Fig. 14.

Our bar chart analysis for the dissolution feature demonstrates that velocity increases as dissolution increases for low porosity samples (classes 1 to 3) (Fig. 15). Nevertheless, the trend changes for the high porosity samples (classes 4 and 5) as the velocity decreases with increasing dissolution. In other words, dissolution enhances the velocities in classes 1 to 3 (porosity ranges from 0 to 13.854%), then caused the velocities to decrease in higher porosities (porosity ranges from 13.854 to 23.09%). The incremental effect of dissolution on acoustic velocities in classes 1 to 3 can be related to the creation of moldic and vuggy isolated pores. In the last two porosity classes

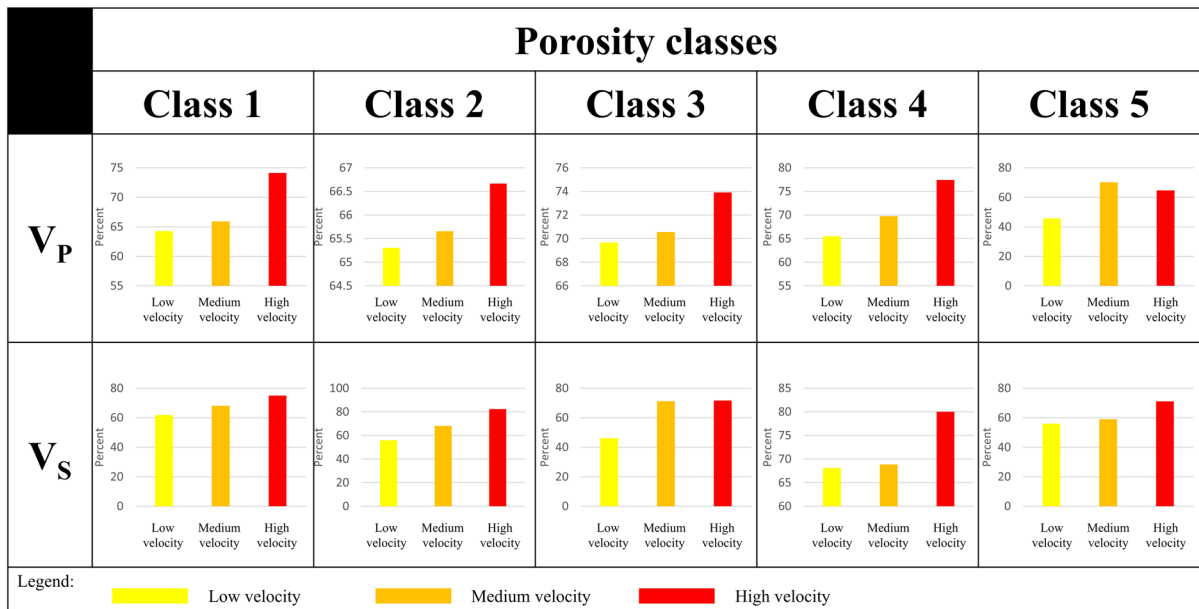


Fig. 13 The percentage of samples that underwent compaction to total investigated samples for different velocity groups (low, medium, and high velocities) in each porosity class (classes one to five)

(high porosities), moldic and vuggy pores are not isolated and are connected to other pores, therefore, their structure is not as stiff as an isolated circular pore. This along with the effect of higher sample porosity (which is more evident in this porosity range) causes the velocities of these samples to decline. Our observation of the dissolution effect on acoustic velocities for classes 1 to 3 is in accordance with the observations of Fabricius (2003) and Salih et al. (2021a).

4.1 Micritization

This feature was evidenced in the Sarvak interval as a dominant diagenetic process. Figure 16 illustrates four thin section views of micritization process in the studied samples.

The micritization process presented with a dominance between one to four in our examined samples (Fig. 10). However, there are intervals without the micritization process. Therefore, we calculated the percentage of the samples with micritization to the total studied samples in different velocity groups within each porosity class. Figure 17 depicts the results of micritization effects on velocity variations. This figure illustrates that micritization caused the velocity to decrease in the examined formation.

This velocity reduction can be linked to the porosity enhancement caused by micritization.

4.2 Open fracturing

Fracturing is a common diagenetic process in carbonate sediments that significantly improve permeability and reservoir quality of our reservoir rock (Matonti et al. 2015). In many cases, fractures were filled (completely or partially) by calcite cement. Meanwhile, open fractures were also present, and their influence on sonic velocities has been investigated in this study. Figure 18 indicates the thin section images of fracture feature occurrence in the examined samples.

In general, the impact of fracturing on sonic wave velocities was reported as a reducing effect in the literature (Anselmetti and Eberli 1993; Matonti et al. 2015). In this research, we analyzed thin section and SEM data and identified open fracturing dominance in each sample group. Open fractures existed only with the dominance of one in our studied samples, while there were intervals in which open fractures were not detected (Fig. 10). Bar chart analysis was performed on the open fracturing feature, and the results are presented in Fig. 19. The general trends indicate velocity reduction by increasing the

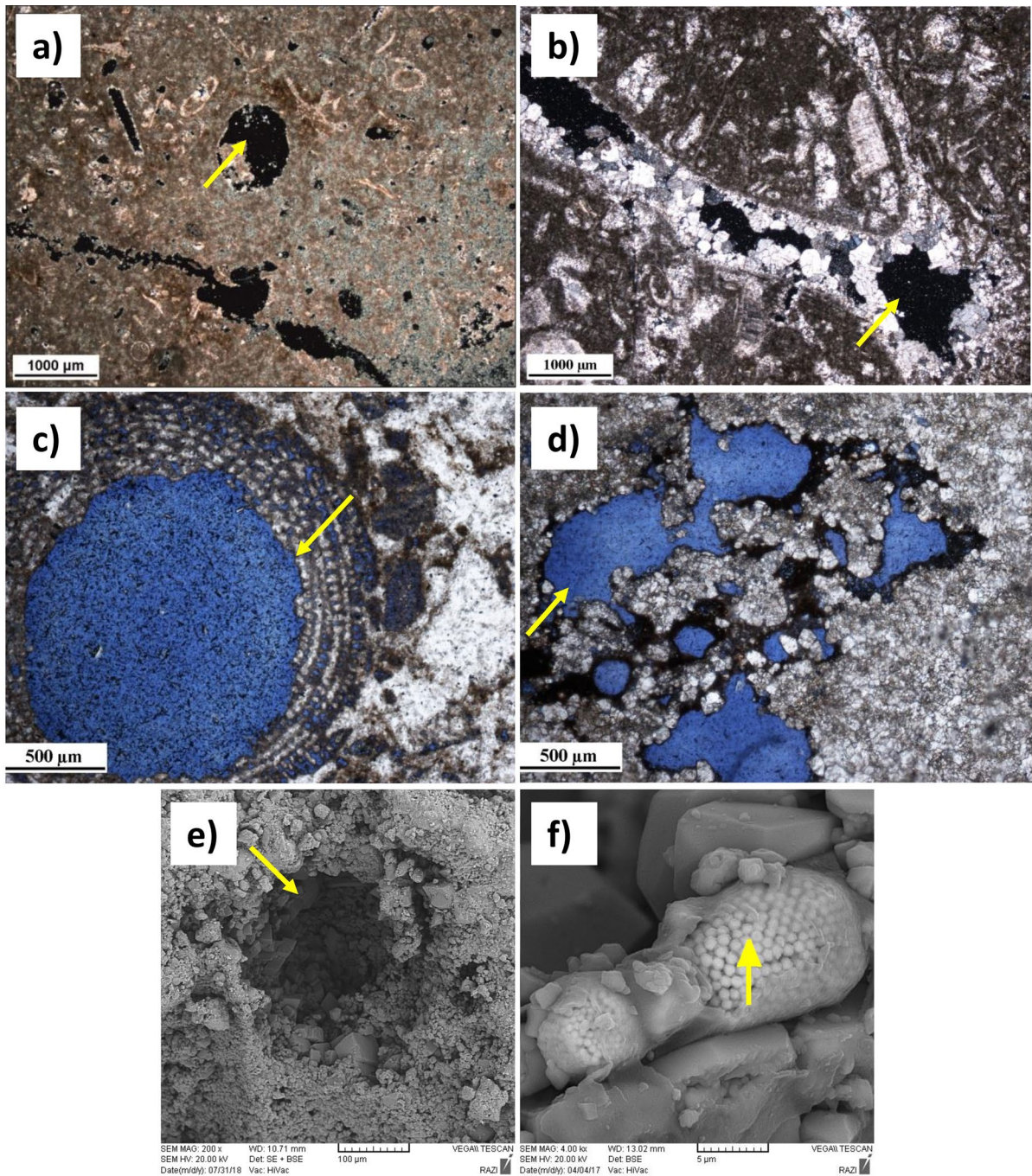


Fig. 14 Photomicrographs and SEM images of dissolution features in the Sarvak formation. **a** dissolution molds (well W1, depth=2909.74 m), **b** dissolution molds (well W2, depth=2628.39 m), **c** dissolution vugs (well W3, depth=2813.61 m), **d** dissolution molds (well W4,

depth=2743.70 m), **e** SEM photo of dissolution vugs (well W2, depth=2877.91 m), and **f** SEM photo of small cavity formed by dissolution within calcite cement crystals and then was filled by pyrite (well W1, depth=2877.91 m)

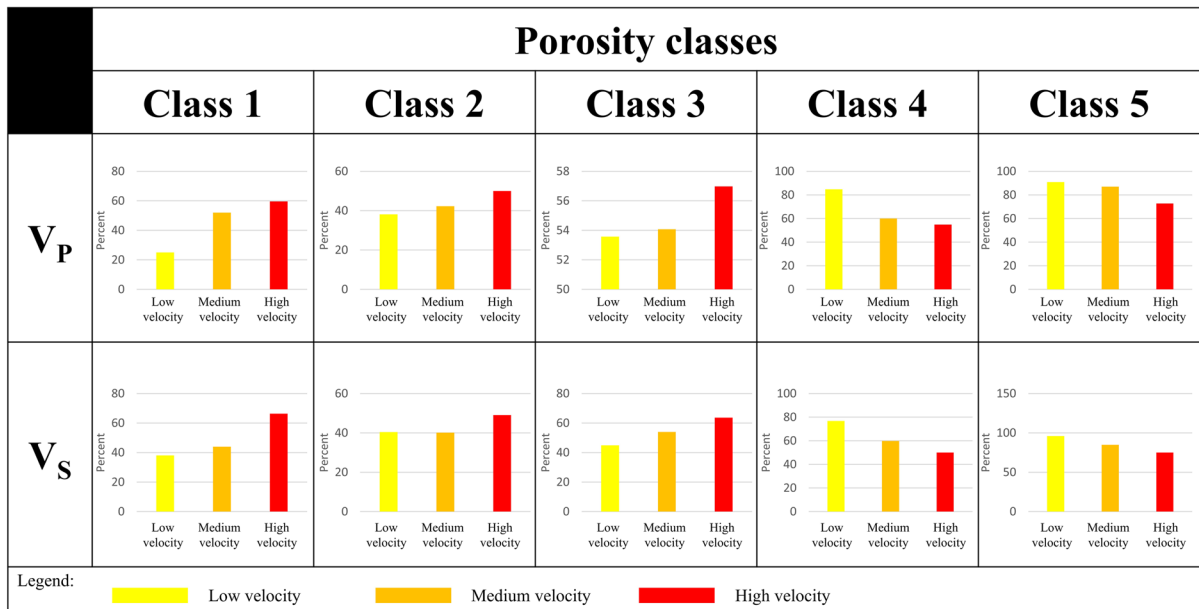


Fig. 15 The percentage of samples that underwent dissolution to total investigated samples for different velocity groups (low, medium, and high velocities) in each porosity class (classes one to five)

dominance of open fractures in each porosity class. In other words, there is a contrary relation between open fracture occurrence and sonic velocity growth. This behavior can be linked to the cracks propagation and rock matrix weakening induced by fracturing. This result is consistent with the results of Anselmetti and Eberli (1993) and Matonti et al. (2015) for the fracturing effects on the acoustic velocities.

4.3 Neomorphism

In the Sarvak formation, recrystallization was the dominant type of neomorphism. There were instances of neomorphism features throughout the studied interval ranging from rarely dominant to highly dominant (Fig. 10). In Fig. 20, thin section images of the neomorphism process are shown.

We applied the bar chart analysis for this diagenetic process, and the results are presented in Fig. 21. According to this figure, the percentage of samples with neomorphism declined as the velocity increased in each porosity class. Therefore, we can conclude that presence of neomorphism reduces velocities in our dataset. Our results are similar to the results of Verwer et al. (2008). This reduction can be linked to

the porosity and permeability enhancement caused by recrystallization.

5 Discussion

Carbonate rocks are geologically complex due to the post-depositional processes that modify their depositional microstructures (Regnet et al. 2019; Salih et al. 2021a, b). This complexity makes their physical properties more heterogeneous and difficult to model and interpret (Regnet et al. 2019). In this study, we investigated different factors affecting sonic velocities using a complete dataset from a carbonate reservoir. The dataset contains well logs, cores, thin section images, XRD analysis, and SEM images.

We observed that the measured velocity is affected by porosity, bioturbation, compaction, dissolution, micritization, open fracture, and neomorphism. However, since mineralogy changes was minimal in the dataset utilized in this study it was not a controlling factor on velocity changes. Overall, we observed that bioturbation and compaction increase the velocities for all porosity ranges, but dissolution increased velocities only for the low and medium porosity samples while reduced them in

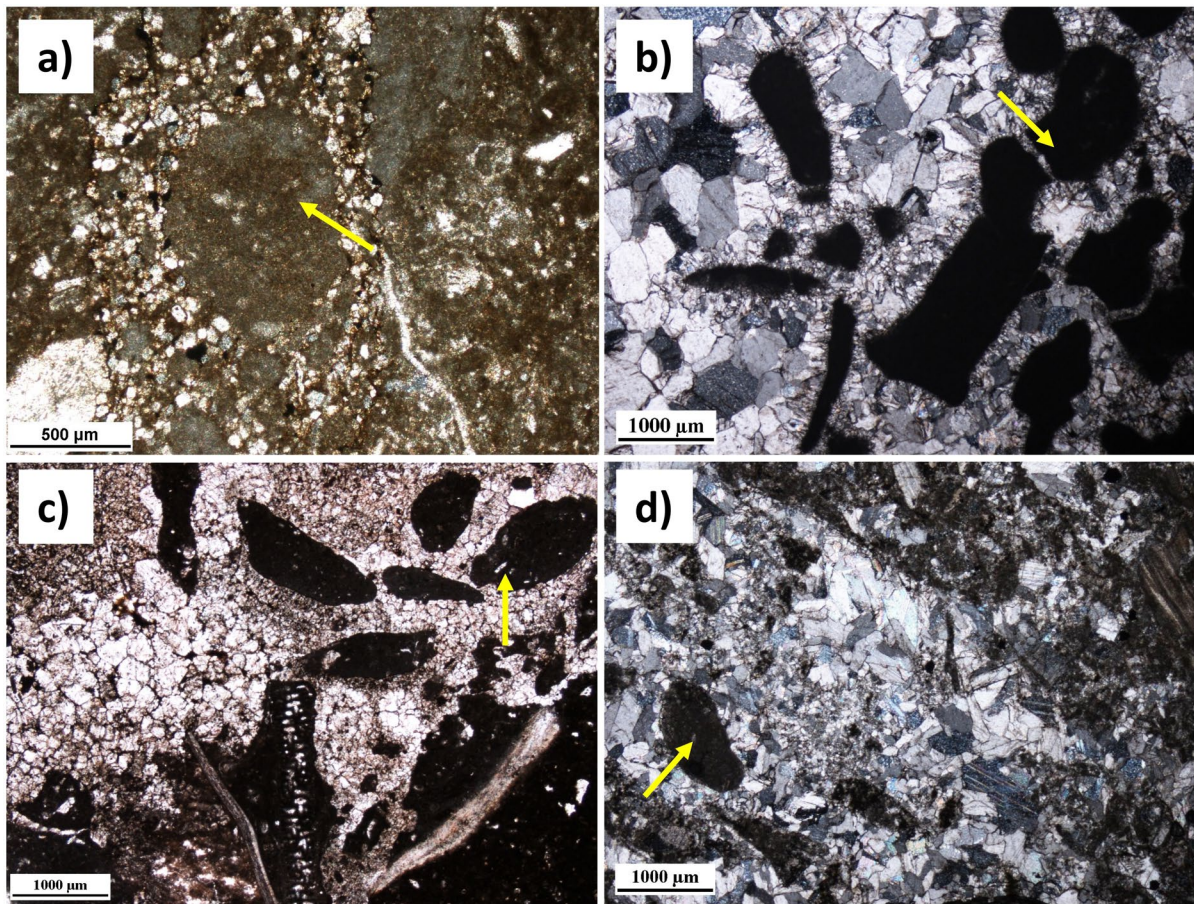


Fig. 16 Photomicrographs of micritization features in the Sarvak formation. **a** Well W1, depth=2726.10 m), **b** well W2, depth=2652.27 m, **c** well W2, depth=2658.13 m, and **d** well W4, depth=2757.17 m)

the high porosity samples. Furthermore, micritization, open fracture, and neomorphism decreased the sonic velocities. This section will discuss the effects of the mentioned controlling factors on sonic velocities in more detail.

It is well known that porosity is the first-order influencing parameter on the sonic velocities in sedimentary rocks, and velocity increases as porosity decreases (Anselmetti and Eberli 1993; Brigaud et al. 2010; Salih et al. 2021a, b; Wyllie et al. 1956). In our dataset, we observed the same trend as decreasing in porosity makes rock stiffer, and as a result, velocity increases (Fig. 8). We observed a strong negative correlation between well-log velocities and porosity ($R_{2_{vp-\phi}} = 0.92$ and $R_{2_{vs-\phi}} = 0.84$), indicating porosity variations adversely change

acoustic velocities as well. When the porosity decreases, the volume fraction of pore space volume decreases, resulting in a rise in the rock mass volume fraction and an increase in the velocity due to the lower elastic properties of fluids compared with minerals. We also investigated the relationship between velocity variations and interpreted pore types. These pore types are interpreted visually from thin sections and SEM images. We did not find any meaningful relationship between these interpreted pore shapes and velocity variations. This could be due to the fact that velocity sees stiffness of the pore space which necessarily does not link to the observed shapes on the images (like contact cementation at grain contacts which can strengthen interparticle porosity to be seen as stiff or round

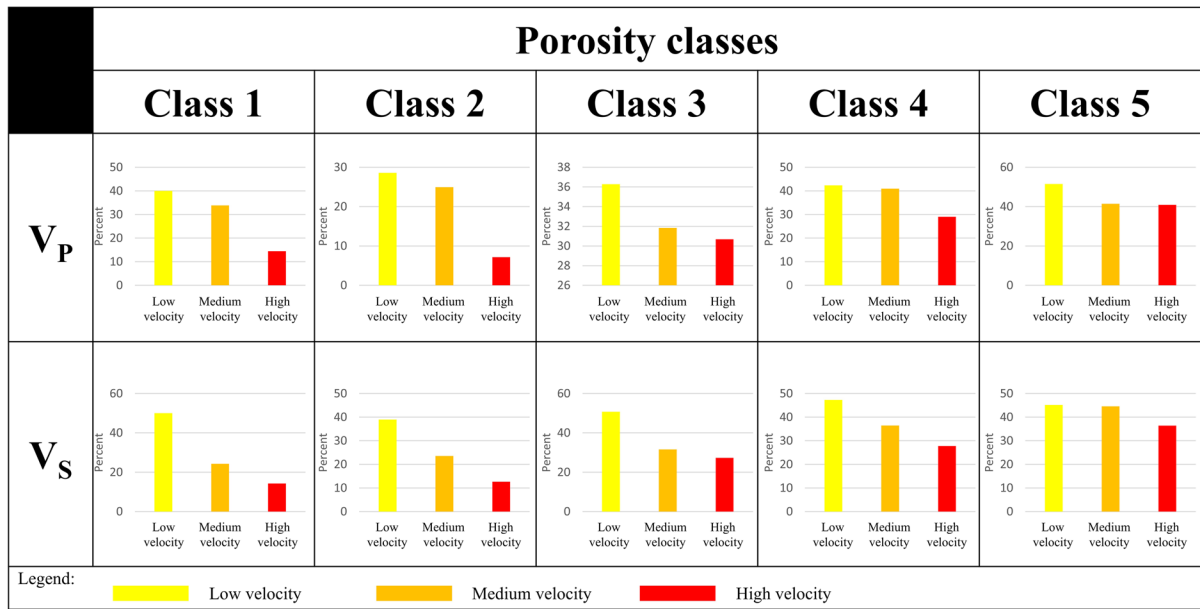


Fig. 17 The percentage of samples that underwent micritization to total investigated samples for different velocity groups (low, medium, and high velocities) in each porosity class (classes one to five)

pores on velocity data). We will investigate this through different diagenetic process which are the source of different pore geometries. Therefore, we continue our study with the effects of different diagenetic processes.

First, bioturbation effects were analyzed and an increase in velocities with intensifying bioturbation was observed (Fig. 11). According to the examined samples, bioturbation occurred in the forms of the burrow and boring. Afterward, pores were filled with peloids, micrite, and cement, strengthening the rock. Therefore, the main reason that the bioturbation process caused velocity growth can be linked to its filling with stiff minerals. It has been demonstrated that the effect of the bioturbation process on acoustic velocities is dependent upon the burrow filling materials in a study by Salih et al. (2021b). According to their findings, fine grain-filled burrows have lower porosity and higher velocity than coarse grain-filled burrows (Salih et al. 2021b). In addition, the bioturbation process can generate pores with a strong structure (high aspect ratio) (Fig. 9), which may result in rock strengthening and increasing in velocity.

Then, we continued with the compaction effects and found out that compaction increases velocities (Fig. 13). Both mechanical and chemical

compactions were evidenced in the Sarvak formation (Fig. 12). In the shallow depths, overburden weights on the sediments lead to the mechanical compaction process and porosity reduction (Croizé et al. 2013). In deeper burials, chemical compaction is dominant due to the excessive applied stress that causes pressure solution at grains contacts (Croizé et al. 2013). Fluid presence also assists this process by contributing to the compaction and fragmentation of the grains by rearrangement of the particles. Mechanical compaction was one of the main porosity-reducing diagenetic processes in the Sarvak formation. On the other hand, chemical compaction does not considerably affect pore volume, since pressure dissolution mainly happens at the grain boundaries (ignoring external cement sources). Some researchers claimed that stylolite could create a flow path and increase permeability (Heap et al. 2014; Mehrabi et al. 2016). Nevertheless, it is not still firmly proven, and more studies need to be performed to verify this hypothesis (Bruna et al. 2019). Consequently, it can be said that mechanical compaction can affect acoustic velocities more than chemical compaction (ignoring introduction of external cement into the sediments). In general, compaction mechanisms reduced the porosity and

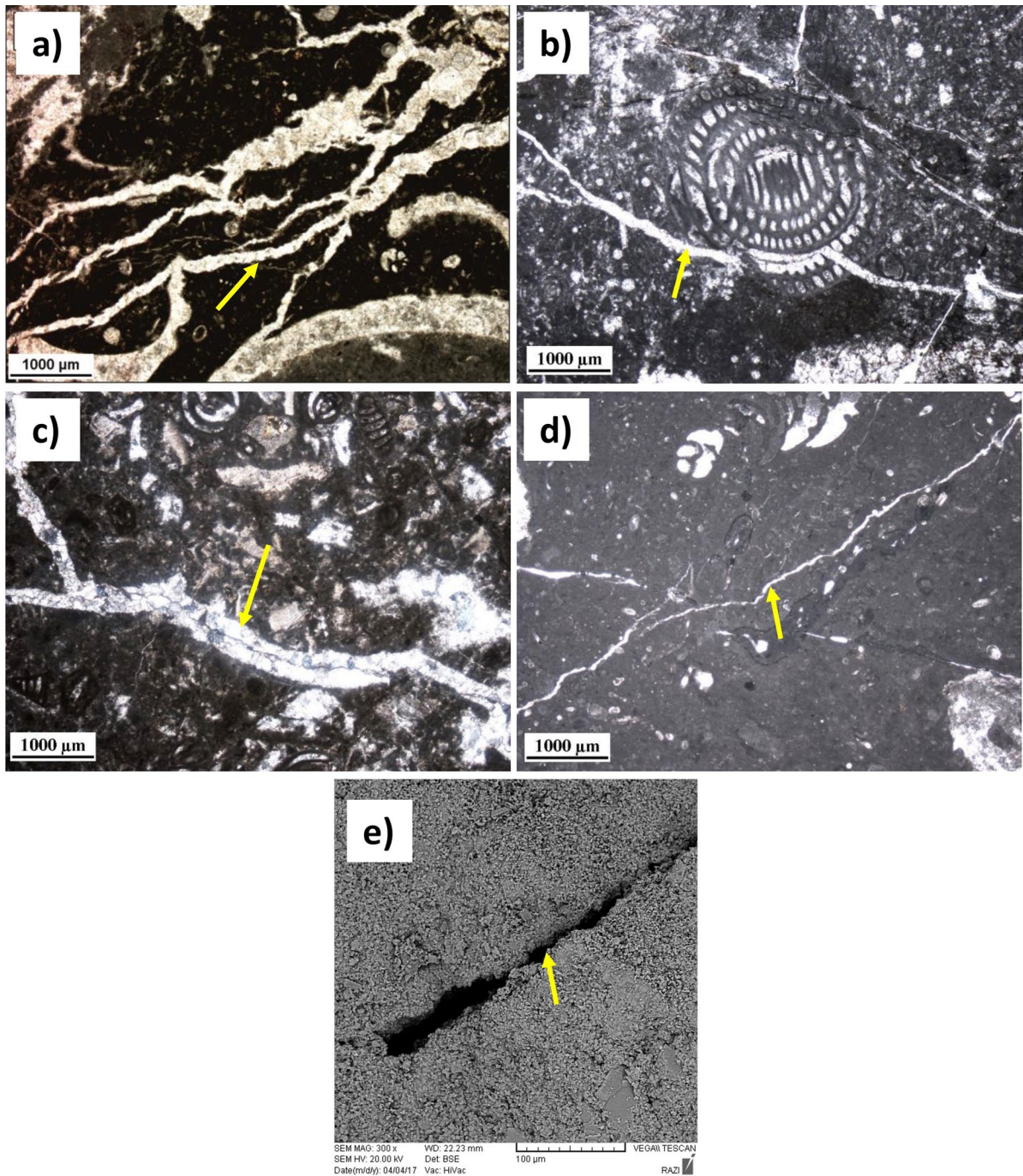


Fig. 18 Photomicrographs of fracturing features in the Sarvak formation. **a** Open fractures (well W1, depth=2814.23 m), **b** partially filled fracture (well W2, depth=2650.64 m), **c** filled

fracture (well W3, depth=2745.20 m), **d** open fracture (well W4, depth=2773.50 m), and **e** SEM image of open fractures partially enlarged by dissolution (well W1, depth=2720.90 m)

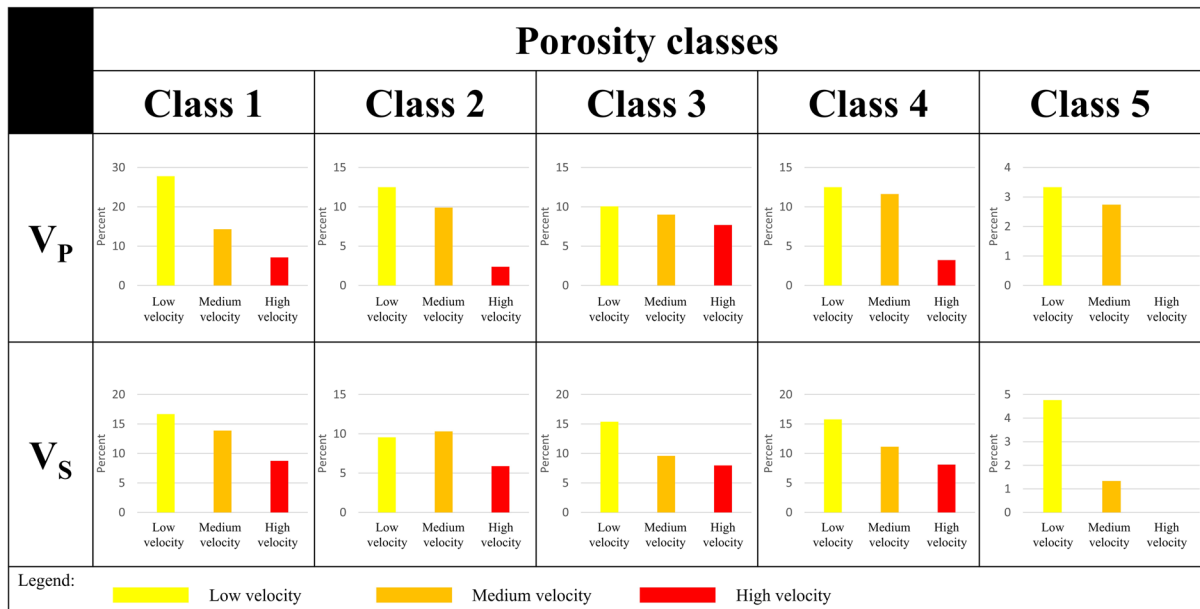


Fig. 19 The percentage of samples that underwent open fracturing to total investigated samples for different velocity groups (low, medium, and high velocities) in each porosity class (classes one to five)

increased acoustic velocities in the Sarvak formation. This result is in line with the findings of Brigaud et al. (2010) and Jaballah et al. (2021).

We continued our investigation by taking dissolution into account. We observed that dissolution effects are dependent on the porosity of the samples. In our dataset, sonic velocities increased by the occurrence of the dissolution feature in the porosities lower than 13.854% (Fig. 14). In classes 1 to 3 (Porosity < 13.854%), the dissolution process creates isolated stiff pores (moldic and vuggy) with a strong structure (aspect ratio close to 1), leading to the rock strengthening and velocity increase for the low porosity samples. Velocity increase by the dissolution feature has already been reported by Fabricius (2003) and Salih et al. (2021a). However, in classes 4 and 5 (high porosity samples between 13.854 and 23.09%), the dissolution dominance caused the velocity to decrease (Fig. 14). Indeed, in this porosity group, generated secondary porosity does not stiffen the rock because the created pores interconnect separated pores and enlarge pore throat size, resulting in the development of soft pores (aspect ratio close to 0), permeability enhancement, and consequently velocity reduction. Here, we observe that dissolution can affect velocity differently in low and high porosity

samples in terms of the new generated porosities and pore shapes. It seems that in the higher porosity samples the effects of this porosity enhancement is more dominant compared with the effects of the generated pore shapes. Furthermore, we analyzed dissolution and bioturbation processes together to ensure the trend reversal observed in the dissolution. In this regard, the percentage of the samples containing both bioturbation and dissolution features to the total examined specimens were calculated for various velocity groups in each porosity class, and bar chart analysis was conducted. The bar chart diagrams for specimens with both dissolution and bioturbation processes are displayed in Fig. 22. It can be seen that the velocity trend again has changed between classes three and four, which confirms our previous results.

The micritization process was observed in the Sarvak formation as another main diagenetic process with dominance between 0 and 4 (Fig. 10). We observed that it reduces sonic velocities (Fig. 17). It normally occurs during compaction (Chafeet et al. 2020; Taghavi et al. 2006), and to some extent, inhibits porosity reduction of the rock due to compressive stress applied to them during compaction (Chafeet et al. 2020; Taghavi et al. 2006). This process can cause porosity increases in the micritized deposits

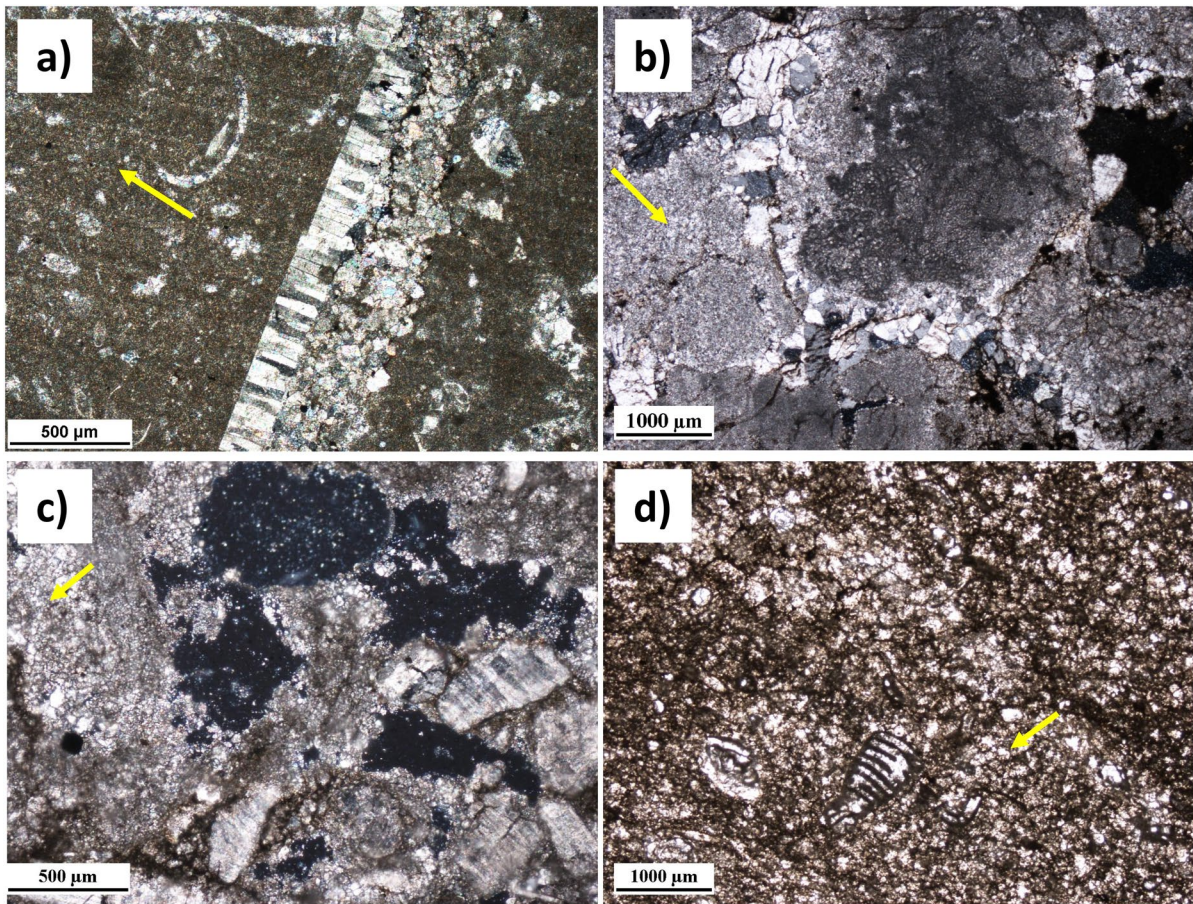


Fig. 20 Photomicrographs of neomorphism or recrystallization features in the Sarvak formation. **a** Well W1, depth=2720.66 m), **b** well W2, depth=2613.54 m, **c** well W4, depth=2739.81 m, and **d** well W4, depth=2767.59 m)

compared with non-micritized sediments. As a result, we observed lower acoustic velocities in the rocks that underwent the micritization process compared to the samples without this diagenetic feature.

Fractures were recorded as important post-depositional (diagenetic) and tectonic features in the Sarvak formation (Fig. 10). Open micro-fractures generate crack pores (pores with a small aspect ratio) in the rock which in turn can significantly reduce the acoustic velocities of the rock (Eberli et al. 2003). We observed the same trend in our dataset (Fig. 19). Open fractures in a rock can generally delay waveform propagation and change its amplitude (Boadu and Long 1996). The intensity of the delayed time and amplitude reduction of the waveform can differ based on the fracture parameters (Boadu and Long 1996). This time delay reduces the acoustic velocities, like what we

had observed in Fig. 19. Other publications have also mentioned that fractures reduce sonic wave velocities (Gregor P Eberli et al. 2003; Matonti et al. 2015).

In order to ensure fracture and micritization reducing impact on acoustic velocities, we conducted the bar chart on the samples that have both of these features, similar to what we did for dissolution and bioturbation processes, and the results are displayed in Fig. 23. It is obvious that the specimens with a higher percentage of micritization and open fracturing features have lower velocities compared with other samples. In other words, the percentage of micritized and open fractured samples declined by the velocity increase in each porosity class. This analysis results have confirmed the abovementioned results that open fractures and micritization reduce velocities.

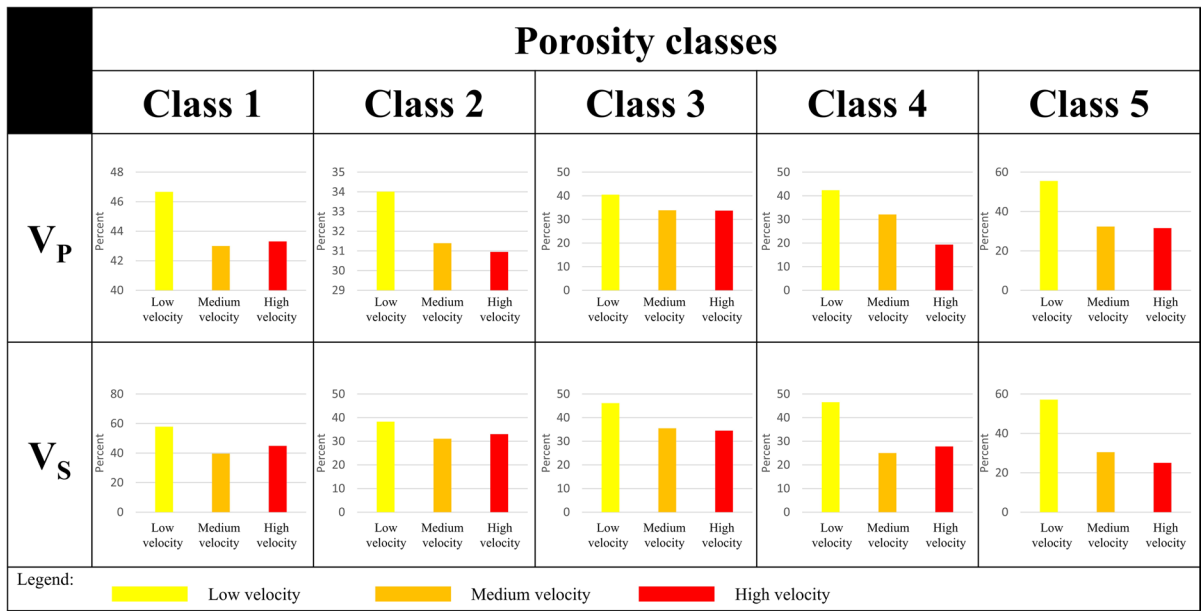


Fig. 21 The percentage of samples that underwent neomorphism to total investigated samples for different velocity groups (low, medium, and high velocities) in each porosity class (classes one to five)

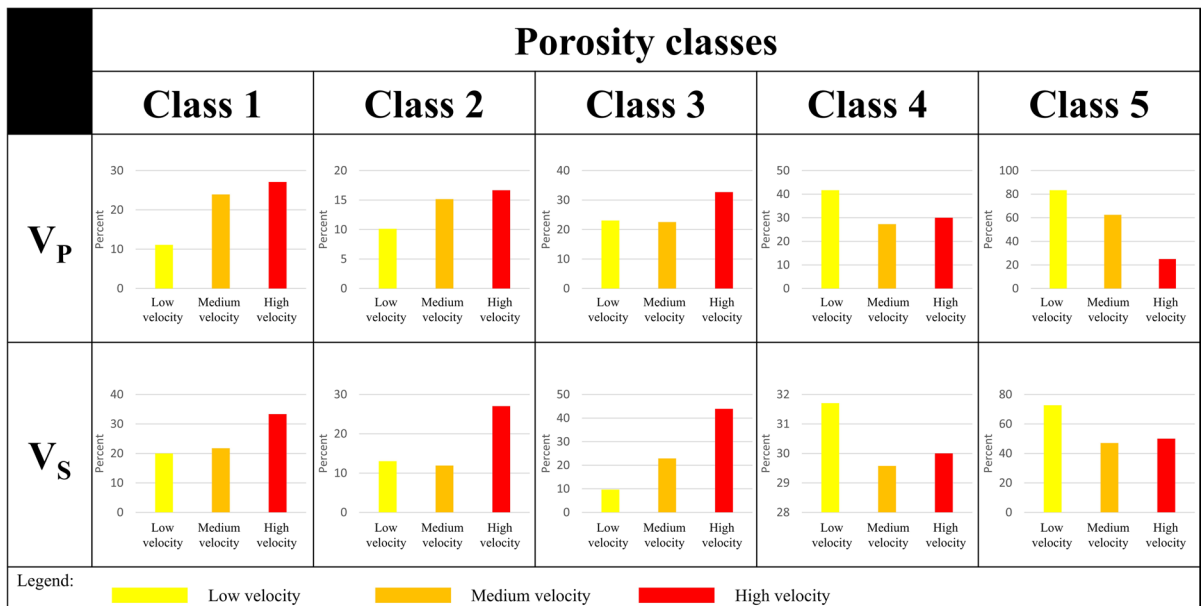


Fig. 22 The percentage of samples that underwent both dissolution and bioturbation processes to total investigated samples for different velocity groups (low, medium, and high velocities) in each porosity class (classes one to five)

The neomorphism process is another dominant diagenetic process in the studied samples from the Sarvak formation (Fig. 10). Our observations

revealed that the existence of this feature reduces sonic velocities (Fig. 21). In the Sarvak formation, the neomorphism process caused recrystallization

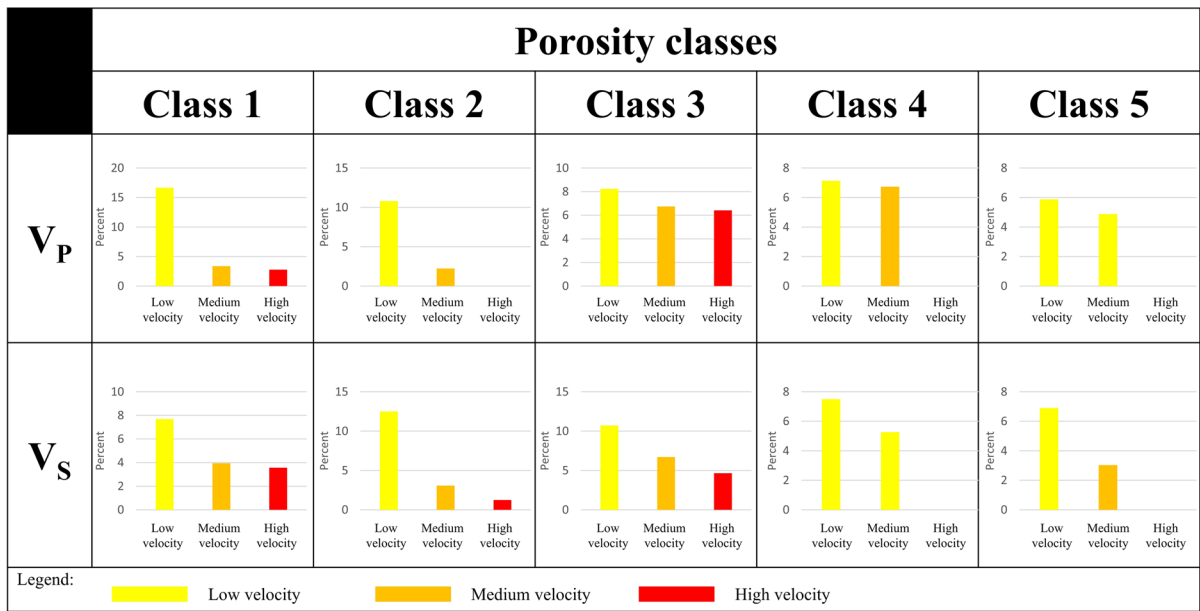


Fig. 23 The percentage of samples that underwent both micritization and open fracturing processes to total investigated samples for different velocity groups (low, medium, and high velocities) in each porosity class (classes one to five)

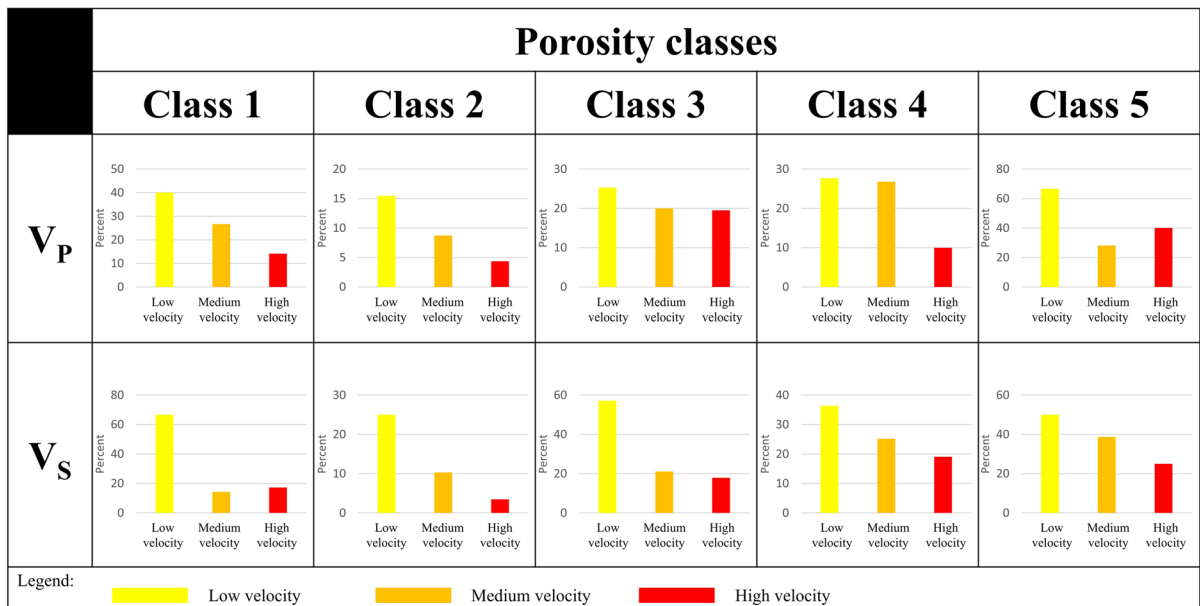


Fig. 24 The percentage of samples that underwent both micritization and neomorphism processes to total investigated samples for different velocity groups (low, medium, and high velocities) in each porosity class (classes one to five)

feature, leading to microporosity developments (Deweever et al. 2007; Moshier 1989). It is well known that porosity has an inverse relationship

with velocity. Therefore, it can be said that neomorphism process leads to velocity reduction (Fig. 21). Our results on the acoustic velocities

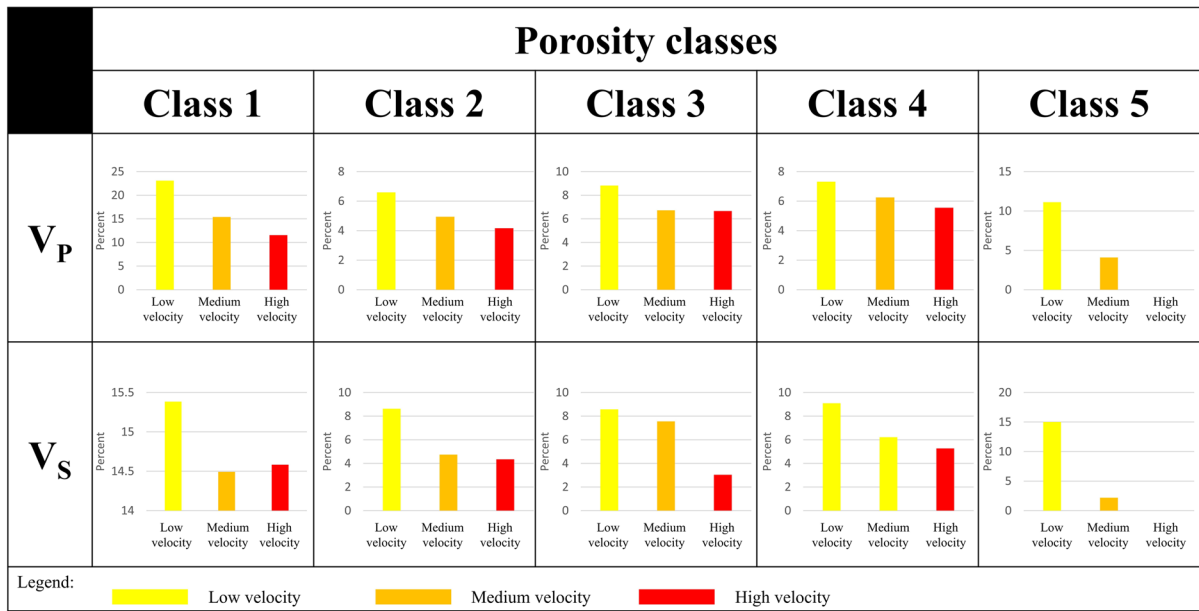


Fig. 25 The percentage of samples that underwent both open fracturing and neomorphism processes to total investigated samples for different velocity groups (low, medium, and high velocities) in each porosity class (classes one to five)

with neomorphism are in line with the results of Verwer et al. (2008).

In addition, we investigated the neomorphism process with micritization and open fracture processes. In this regard, bar chart analysis was performed, and the result of micritization and neomorphism features are displayed in Fig. 24. Generally, in each porosity class, it is evident that the percentage of samples with both neomorphism and micritization is higher in low velocities (the percentage decreases with velocity growth). Therefore, obtained results for micritization and neomorphism impacts on acoustic velocities have been confirmed.

A similar analysis was conducted for the open fracture and neomorphism processes that is presented in Fig. 25. According to the bar chart trends in each porosity class, neomorphism and open fracture percentages decreased with velocity increase, as expected.

6 Conclusions

This study looked into the elements that influence sonic velocities in the Sarvak formation of an oil field in Iran’s Abadan plain. The dataset, which included

well logs, cores, and drilling cuttings, was evaluated utilizing a variety of techniques such as XRD analysis, thin section analysis, and SEM imaging.

The mineralogical analysis revealed that calcite comprises more than 95% of the examined samples on average, followed by dolomite, the second most prevalent mineral. Due to the negligible proportion of clay minerals in the samples analyzed for this study and the similarity of the elastic properties of dolomite and calcite, it can be concluded that mineralogy does not have significant effect on the velocity fluctuations observed in this study.

Different diagenetic processes in the Sarvak formation were found using SEM images and thin-section data analysis. To reduce the impact of porosity differences on sonic wave velocities, the data was separated into five porosity classes for further research.

Bioturbation increased velocities, which can be linked to the formation of stiff pores and their subsequent filling with stiff minerals during the bioturbation process. Because of the loss of porosity, mechanical and chemical compaction increased sonic velocities. The effect of dissolution on sonic velocities was affected by sample porosity. Dissolution formed isolated stiff pores in lower porosity levels, resulting in rock strengthening and velocity increase. However,

dissolution dominance produced a decrease in velocity in higher porosity ranges due to the growth of soft pores and connections between separated pores.

Sonic velocities were shown to be reduced by micritization, open fracture, and neomorphism. Porosity reduction was suppressed during compaction by micritization, resulting in greater velocities in micritized samples. Open fracturing created low aspect ratio cracks, which reduced velocity. Neomorphism, predominantly in the form of recrystallization, led in the formation of microporosity and, as a result, a decrease in sonic velocities.

In conclusion, our work sheds light on the processes that influence sonic velocities in the Sarvak formation. The results emphasize the importance of porosity changes and other diagenetic processes in influencing sonic velocity behavior. These findings add to a better knowledge of reservoir characteristics and can benefit in the interpretation of seismic waves.

Author contributions Conceptualization: MHK, MEN, MRS; Methodology: MHK, MRS; Formal analysis and investigation: MHK, MRS; Writing—original draft preparation: MHK; Writing—review and editing: MEN, MRS; Resources: MEN; Software and coding: MHK; Validation: MEN; Supervision: MEN, MRS.

Funding The authors did not receive support from any organization for the submitted work.

Availability of data and materials Data sharing not applicable.

Declarations

Ethics approval and consent to participate Not applicable.

Consent for publication Not applicable.

Competing interests The authors declare no competing interests.

Open Access This article is licensed under a Creative Commons Attribution 4.0 International License, which permits use, sharing, adaptation, distribution and reproduction in any medium or format, as long as you give appropriate credit to the original author(s) and the source, provide a link to the Creative Commons licence, and indicate if changes were made. The images or other third party material in this article are included in the article's Creative Commons licence, unless indicated otherwise in a credit line to the material. If material is not included in the article's Creative Commons licence and your intended use is not permitted by statutory regulation or exceeds

the permitted use, you will need to obtain permission directly from the copyright holder. To view a copy of this licence, visit <http://creativecommons.org/licenses/by/4.0/>.

References

- Anselmetti FS, Eberli GP (1993) Controls on sonic velocity in carbonates. *Pure Appl Geophys* 141(2):287–323
- Assadi A, Honarmand J, Moallemi S-A, Abdollahie-Fard I (2016) Depositional environments and sequence stratigraphy of the Sarvak Formation in an oil field in the Abadan Plain. *SW Iran Facies* 62(4):1–22
- Assadi A, Honarmand J, Moallemi SA, Abdollahie-Fard I (2018) An integrated approach for identification and characterization of palaeo-exposure surfaces in the upper Sarvak Formation of Abadan Plain, SW Iran. *J Afr Earth Sc* 145:32–48
- Boadu FK, Long LT (1996) Effects of fractures on seismic-wave velocity and attenuation. *Geophys J Int* 127(1):86–110
- Brigaud B, Vincent B, Durlot C, Deconinck J-F, Blanc P, Trouiller A (2010) Acoustic properties of ancient shallow-marine carbonates: effects of depositional environments and diagenetic processes (Middle Jurassic, Paris Basin, France). *J Sediment Res* 80(9):791–807
- Bruna P-O, Lavenu APC, Matonti C, Bertotti G (2019) Are stylolites fluid-flow efficient features? *J Struct Geol* 125:270–277
- Bullock P, Fedoroff N, Jongerius A, Stoops G, Tursina T (1985) Handbook for soil thin section description. *Waine Research*
- Chafeet HA, Raheem MK, Dahham NA (2020) Diagenesis processes impact on the carbonate Mishrif quality in Ratawi oilfield, southern Iraq. *Model Earth Syst Environ* 6(4):2609–2622
- Croizé D, Bjørlykke K, Jähren J, Renard F (2010) Experimental mechanical and chemical compaction of carbonate sand. *J Geophys Res Solid Earth*. <https://doi.org/10.1029/2010JB007697>
- Croizé D, Renard FF, Gratier J-P, Croize D, Renard FF, Gratier J-P (2013) Compaction and porosity reduction in carbonates: a review of observations, theory, and experiments. In: Dmowska G (ed) *Advances in geophysics*, vol 54. Elsevier, Amsterdam, pp 181–238. <https://doi.org/10.1016/B978-0-12-380940-7.00003-2>
- Deweever B, Breesch L, Mezini A, Swennen R (2007) Sedimentological and marine eogenetic control on porosity distribution in Upper Cretaceous carbonate turbidites (central Albania). *Sedimentology* 54(2):243–264
- Dickson JAD (1966) Carbonate identification and genesis as revealed by staining. *J Sediment Res* 36(2):491–505
- Du Y, Chen J, Cui Y, Xin J, Wang J, Li Y-Z, Fu X (2016) Genetic mechanism and development of the unsteady Sarvak play of the Azadegan oil field, southwest of Iran. *Pet Sci* 13(1):34–51
- Eberli GP, Baechle GT, Anselmetti FS, Incze ML (2003) Factors controlling elastic properties in carbonate sediments and rocks. *Lead Edge* 22(7):654–660

- El Husseiny A, Vanorio T (2015) The effect of micrite content on the acoustic velocity of carbonate rocks. *Geophysics* 80(4):L45–L55
- Emami Niri M, Mehmandoost F, Nosrati H (2021) Pore-type identification of a heterogeneous carbonate reservoir using rock physics principles: a case study from south-west Iran. *Acta Geophys* 69(4):1241–1256
- Esrāfilī-Dizajī B, Rahimpour-Bonab H, Mehrabi H, Afshin S, Kiani Harchegani F, Shahverdi N (2015) Characterization of rudist-dominated units as potential reservoirs in the middle Cretaceous Sarvak Formation. *SW Iran Facies* 61(3):1–25
- Fabricius IL (2003) How burial diagenesis of chalk sediments controls sonic velocity and porosity. *AAPG Bull* 87(11):1755–1778
- Grélaud C, Razin P, Homewood P (2010) Channelized systems in an inner carbonate platform setting: differentiation between incisions and tidal channels (Natih Formation, Late Cretaceous, Oman). *Geol Soc Lond Spec Publ* 329(1):163–186
- Hafner B (2007) Scanning electron microscopy primer. Characterization Facility, University of Minnesota-Twin Cities, pp 1–29
- Heap MJ, Baud P, Reuschlé T, Meredith PG (2014) Stylolites in limestones: barriers to fluid flow? *Geology* 42(1):51–54
- Jaballah J, Reijmer JGG, El-Husseiny A, Le Goff J, Hairabian A, Slooman A (2021) Physical properties of Cretaceous to Eocene platform-to-basin carbonates from Albania. *Mar Pet Geol* 128:105022
- Jafarian E, Kleipool LM, Scheibner C, Blomeier DPG, Reijmer JGG (2017) Variations in petrophysical properties of Upper Palaeozoic mixed carbonate and non-carbonate deposits, Spitsbergen, Svalbard Archipelago. *J Pet Geol* 40(1):59–83
- James GA, Wynd JG (1965) Stratigraphic nomenclature of Iranian oil consortium agreement area. *AAPG Bull* 49(12):2182–2245
- Jooybari A, Rezaie P (2017) Petrophysical evaluation of the Sarvak Formation based on well logs in Dezful Embayment, Zagros Fold Zone, south west of Iran. *Eng Technol Appl Sci Res* 7(1):1358–1362
- Khosravi MH, Saberi MR, Niri ME (2022) Investigating the effects of reservoir properties and diagenetic features on carbonates velocity variations: a case study. In: 83rd EAGE annual conference and exhibition, vol 2022, pp 1–5. European Association of Geoscientists & Engineers
- Matonti C, Guglielmi Y, Viseur S, Bruna PO, Borgomano J, Dahl C, Marié L (2015) Heterogeneities and diagenetic control on the spatial distribution of carbonate rocks acoustic properties at the outcrop scale. *Tectonophysics* 638:94–111
- Mavko G, Mukerji T, Dvorkin J (2009) The rock physics handbook. <https://doi.org/10.1017/cbo9780511626753>
- Mehrabi H, Rahimpour-Bonab H (2014) Paleoclimate and tectonic controls on the depositional and diagenetic history of the Cenomanian–early Turonian carbonate reservoirs, Dezful Embayment. *SW Iran Facies* 60(1):147–167
- Mehrabi H, Rahimpour-Bonab H, Hajikazemi E, Jamalian A (2015) Controls on depositional facies in Upper Cretaceous carbonate reservoirs in the Zagros area and the Persian Gulf, Iran. *Facies* 61(4):1–24
- Mehrabi H, Mansouri M, Rahimpour-Bonab H, Tavakoli V, Hassanzadeh M (2016) Chemical compaction features as potential barriers in the Permian-Triassic reservoirs of Southern Iran. *J Petrol Sci Eng* 145:95–113
- Moshier SO (1989) Microporosity in micritic limestones: a review. *Sed Geol* 63(3–4):191–213
- Motiei H (1993) Stratigraphy of Zagros. Geological survey of Iran. *Farsi*, 536
- Rahimpour-Bonab H, Mehrabi H, Enayati-Bidgoli AH, Omidvar M (2012a) Coupled imprints of tropical climate and recurring emergence on reservoir evolution of a mid Cretaceous carbonate ramp, Zagros Basin, southwest Iran. *Cretac Res* 37:15–34
- Rahimpour-Bonab H, Mehrabi H, Navidtalab A, Izadi-Mazidi E (2012b) Flow unit distribution and reservoir modelling in cretaceous carbonates of the Sarvak Formation, Abteymour Oilfield, Dezful Embayment, SW Iran. *J Pet Geol* 35(3):213–236
- Raymer LL, Hunt ER, Gardner JS (1980) An improved sonic transit time-to-porosity transform. In: SPWLA 21st annual logging symposium. OnePetro
- Regnet JB, David C, Robion P, Menéndez B (2019) Microstructures and physical properties in carbonate rocks: a comprehensive review. *Mar Pet Geol* 103:366–376
- Saberi MR (2020) Geology-guided pore space quantification for carbonate rocks. *First Break* 38(3):49–55
- Salih M, Reijmer JGG, El-Husseiny A (2021a) Diagenetic controls on the elastic velocity of the early Triassic Upper Kharitam Member (Khuff Formation, central Saudi Arabia). *Mar Pet Geol* 124:104823
- Salih M, Reijmer JGG, El Husseiny A, Bashri M, Eltom H, Mukainah HA, Kaminski MA (2021b) Controlling factors on petrophysical and acoustic properties of bioturbated carbonates: (Upper Jurassic, Central Saudi Arabia). *Appl Sci* 11(11):5019
- Serra OE (1983) Fundamentals of well-log interpretation
- Setudehnia A (1978) The mesozoic sequence in south-west Iran and adjacent areas. *J Pet Geol* 1(1):3–42
- Taghavi AA, Mørk A, Emadi MA (2006) Sequence stratigraphically controlled diagenesis governs reservoir quality in the carbonate Dehluran Field, southwest Iran. *Pet Geosci* 12(2):115–126
- Verwer K, Braaksma H, Kenter JA (2008) Acoustic properties of carbonates: effects of rock texture and implications for fluid substitution. *Geophysics* 73(2):B51–B65
- Wyllie MRJ, Gregory AR, Gardner LW (1956) Elastic wave velocities in heterogeneous and porous media. *Geophysics* 21(1):41–70
- Xu S, Payne MA (2009) Modeling elastic properties in carbonate rocks. *Lead Edge* 28(1):66–74
- Zhou W, Apkarian R, Wang ZL, Joy D (2007) Fundamentals of scanning electron microscopy (SEM). In: Scanning microscopy for nanotechnology: techniques and applications, pp 1–40

Publisher's Note Springer Nature remains neutral with regard to jurisdictional claims in published maps and institutional affiliations.